An Imaging Fourier Transform Spectrometer for the Next Generation Space Telescope

CSA funded NGST IFTS study – Final Report

Simon Morris and John Ouellette
Herzberg Institute of Astrophysics and National Research Council of Canada.

André Villemaire, Frédéric Grandmont and Louis Moreau
Bomem inc.

1 October 1999

Contents

1. Executive Summary

Bomem and the Herzberg Institute of Astrophysics (HIA) are proud to present their contribution to the Next Generation Space Telescope (NGST) instrument team reports. In the course of our work we studied an Imaging Fourier Transform Spectrometer (IFTS) as the main ISIM instrument for NGST. This document presents the concept of the instrument, an overview of its scientific capabilities as well as trade studies, performance analyses, a risk analysis and the breadboarding activities performed to test the concept and reduce the associated risks.

The work undertaken by the Bomem/HIA team is complementary to the effort of the IFIRS Team (Graham et al, 1999). While the IFIRS Team looked at the end-to-end applicability of an IFTS for NGST, the technical work in this report focuses on the technological feasibility of the Michelson interferometer sub-system, which is the spectral engine of an IFTS. Nonetheless, the present report can also be viewed as a stand-alone document.

There is a vigorous and healthy debate about what kind of instrument should be aboard NGST, the premier astronomical telescope of the next millennium. Eloquent arguments have been presented about the various advantages and disadvantages of several families of instruments. Some instruments provide the superb imagery necessary to resolve fine spatial features, while others provide the very high spectral resolution to reveal details on the chemical composition of the universe. The IFTS is in a different class, as it provides the great majority of the distinct qualities required to meet the science goals of NGST. The IFTS holds the promise of being the only truly integrated science instrument module (ISIM) and consequently an instrument more effective in terms of mass, volume, cost and scientific return.

As demonstrated in Graham et al. (1999, 1998) and Section 2 of this report, an IFTS can carry out the entire NGST DRM in significantly less time (69%) than the estimated time for the yardstick ISIM. It is also argued that while doing so, the IFTS also provides, at no extra instrument cost, a wealth of scientific data not obtainable with any other single instrument (see Section 2.2.7 for examples).

The advantages of an IFTS are numerous:

1) IFTS provide unrivalled spectroscopy with the lowest level of radiometric errors and absolutely calibrated spectral scales (see Appendix A.2)
2) IFTS provide the best imaging quality, i.e. equivalent to imagers with filters, because a FTS is only composed of a few (as little as three) plane parallel optics.
3) Fourier-transform spectrometers are a relatively mature technology. Several FTS have flown successfully on various space platforms.
4) IFTS require a relatively small number of actuators since the number of moving elements is very limited compared to a multi-object spectrograph (MOS), for instance.
5) IFTS provide broadband coverage, from the visible to the thermal infrared, at adjustable spectral resolution (Panchromatic, R=1, to R > 10000).
6) IFTS have a light gathering advantage over most other types of spectrometers because they do not rely on energy limiting slits.
7) By combining spectral and spatial measurements over a wide field of view, IFTS can carry out simultaneously different science projects.

8) Last but most important, IFTS can survey the complete field of view of NGST and acquire a spectra for every pixel, making them especially appropriate for the unbiased study of uncharted (spectrally and spatially) areas of the sky and making them ideal for fortuitous discoveries.

Most of the above advantages are described in detail in Graham et al. (1998, 1999) and also in Section 2 and 3 of the present document. By contrast, the perceived weaknesses of the IFTS are not as numerous:

1) Less sensitivity at fine spectral resolution than dispersive spectrometers.
2) High technological risk, especially in a space environment.
3) Unproven performances.

Our analysis show that the last two arguments are unfounded and that the first one can be overcome with less effort than is likely to be required to fix other instruments shortcomings[1].

Sensitivity: The summary of the sensitivity analysis can be found in Figure 2 of Graham et al. (1999). It is easy to look at this figure and conclude that an IFTS has a lower sensitivity than a MOS and thus requires a longer total exposure time. This argument is true in some conditions but care must be applied in analysing the assumptions leading to these conditions. First, an IFTS will be photon noise limited most of the time and thus its performance does not rely on predicted detector dark noise; *the NGST IFTS can be built today*. The predicted sensitivity advantage of a MOS quickly relies on the expected future performance of the detectors, and may not be achieved if progress does not come or does not come in time. Second, if the detectors indeed perform as expected, dispersion can be introduced in a FTS instrument as described in Graham et al. (1999) to arrive at a performance equivalent to a MOS and perhaps at a similar level of complexity also. The trade should therefore be centred on the means of getting the spectral discrimination (FT vs. dispersive) rather than around a false association of sensitivity with a particular type of instrument.

When the IFTS is used without dispersion, it can sample the whole field of view while a MOS is limited to a few samples at a time. Depending on the number of objects of interest the apparent FTS sensitivity disadvantage can quickly become a sensitivity advantage because the FTS can stare much longer at the same location in the sky to obtain the number of objects necessary to fulfil the scientific goal. This is illustrated in Section 2.5. Finally the *multiplex "dis-"advantage* of the IFTS: i.e., the fact that the Fourier Transform spreads the noise uniformly across the whole spectral band, must also be considered. This effect will tend to be disadvantageous when observing weak spectral signatures lying besides intense and broadband signal. When we are interested in the detection of the faintest objects however, this situation is not likely because fairly low SNR spectra will be collected and the reduced dynamic range of the FT spectra will not hinder our discrimination ability. In fact this property of the FTS can become an advantage for emission line spectra, where the SNR of the lines will be higher than for a dispersive spectrometer, because the photon noise in the line is spread out over the whole spectral band.

These arguments, like many that have been made by the scientific community in the hope of discriminating between science instruments, are in fact not sufficient to draw a final conclusion. The best way to conduct this instrument trade is to go one step further and perform detailed performance simulations. Based on the accepted set of science goals, the scientists can generate simulated data

[1] We would like to invite the community to communicate any other arguments against the IFTS in order to be able to complete the evaluation of this instrument.

sets for each instrument performance, in order to objectively compare the scientific return per dollar of investment.

Technical risk: Any instrument operating in space, in a cryogenic environment carries an increased level of risk. It is a customary to only consider mature technology for space missions. To some people, the IFTS may seem more risky than other instruments because it is based on interferometry and an interferometric system requires precise alignment of its optical components. The fact is that FTS technology is very much alive today both on the ground and in space, because it has succeeded in solving the "interferometric problem". In fact it is worth noting that the history of FTS in space, initiated almost 40 years ago, has been unusually successful and no example of FTS failure can be cited. FTS have been part of more than 20 space missions, several of them at cryogenic temperature, and more than a dozen FTS are part of future space missions (see Section 3 for an overview). Over these years, a wealth of experience has been gained and strategies, passive and active, have been developed to maintain the alignment during launch and during space operation. Just from this history alone we can say that FTS carries less risk than the more complex and relatively new MOS or IFS (integral field spectrometer) for the space industry.

Unproven performances: Astronomers have not intensively used Fourier transform spectrometers. It may therefore appear to some people that FTS is more "vaporware" than hardware and that performance estimates are based solely on simulations are hence unreliable. In fact, FTS have been intensively used in several fields such as meteorology, planetary survey, environment, etc. For example, FTS are accurate and sensitive enough to measure the fine spectral features and line broadening necessary to estimate with less than 1% error, the vertical profile of humidity and temperature of the atmosphere or to estimate the vertical and horizontal distribution of winds. An example of the exquisite absolute accuracy of FTS is also illustrated in Appendix A.2.

IFTS can deliver unrivalled spectroscopy and imagery for many applications. What can it do for NGST? Bomem/HIA team has concentrated on some of the key science issues and core technological IFTS issues. Firstly, we agree with the IFIRS team and believe that an IFTS can produce a scientific return per dollar that cannot be matched by any other instrument (see Section 2). Secondly our analysis of the technological feasibility indicates that a reliable instrument can be built without great technological feats. This is exemplified by our ongoing effort to build a fully functional breadboard on a short schedule and tight budget (see Section 3.4). The aim of the work described below was to analyse the NGST environment and observational modes, and from this determine the challenges for an IFTS and begin hardware testing to demonstrate solutions to these challenges.

In this report we give an account of the Canadian effort by the HIA/Bomem team to study an IFTS for NGST. Section 2 summarises the analysis of the Galaxy Formation and Evolution part of the NGST Design Reference Mission (DRM). Section 3 summarises the instrument concept development including trade studies, performance analyses and breadboarding activities.

2. Science

2.1 Introduction

In Section 2, we explore some of the pros and cons of using an Imaging Fourier Transform Spectrometer (IFTS) to achieve the scientific goals of the Galaxy Formation and Evolution part of the Next Generation Space Telescope (NGST) Design Reference Mission (DRM). This will be done in four complementary sections. In section 2.2, we will discuss how well matched IFTS observations are to the science goals of the Galaxies DRM. Detailed comparisons of the S/N ratios for IFTS versus MOS observations in the GDRM are listed in section 2.3, along with some discussion of the technical issues. An example of the 'bonus' science obtained from the above approach to the GDRM is given in section 2.4. Finally, a nice summary plot showing some of the pros and cons of IFTS versus MOS observations for the GDRM produced by James Graham is shown in section 2.5. As part of this study, a number of JAVA based web tools were developed by John Ouellette. These tools, including a S/N calculator, are available at http://www.hia.nrc.ca/STAFF/slm/ifts.

2.2 Scientific Gains from an IFTS approach to the Galaxy Formation and Evolution DRM

In this section we will list some of the scientific gains one would obtain by using an IFTS to obtain the data needed for the Galaxy Formation and Evolution parts of the NGST Design Reference Mission (DRM). In particular we will concentrate here on the science gains from obtaining full field 3D spectroscopy.

2.2.1 Science Goals of the Formation and Evolution of Galaxies DRM

The overall science goals for the GDRM are:

1. What were the first sources of light in the Universe?
2. How were galaxies assembled?
3. How did the Hubble Sequence form?
4. How do galaxies interact with their environment?
5. What are the global histories of star formation, metal enrichment and gas consumption?
6. How did the spatial distribution of galaxies evolve?

To achieve these goals, the GDRM proposes a very ambitious six part observing plan, made up of:

1. Deep broad-band imaging in the optical, NIR and MIR for a total of 112 days
2. Deep spectroscopy at R=100 for 100 galaxies, R=1000 for 2500 galaxies, R=5000 for 400 galaxies using a MOS, and IFU observations of 25 galaxies for a total of 118 days.
3. Imaging and Spectroscopy for high redshift clusters, optical and NIR imaging for 10 days, R=1000 and R=5000 MOS spectroscopy for 100 galaxies per cluster in each of 7 clusters, for a total of 31 days.
4. Imaging and spectroscopy of the fields around 8 bright and 8 faint QSOs, with 22 days of optical and NIR imaging, 11 days of R=1000 MOS spectroscopy for 200 galaxies per field, and 11 days of R=5000 MOS spectroscopy for the same sample, giving a total of 66 days.
5. MIR imaging and MOS spectroscopy of a deep field and 16 shallow fields, giving R=300 spectra for a sample of 50 galaxies with highly obscured star formation, taking a total of 64 days (28 days of which overlap with the deep imaging proposal and so need not be counted twice).
6. While all the above is being obtained, the imaging data can be used to search for Supernovae. This links with the SN proposal in the Cosmology section of the DRM, but it is noted in the GDRM that the type IA and II SN rates as a function of redshift are of great interest as a means of charting

the evolution of star formation and metal enrichment in the Universe. These SN would require spectroscopic follow-up and the time for this (if done with a MOS) is listed under the Cosmology DRM.

It should be noted that there are some slight inconsistencies in the hardcopy GDRM proposals, and the above summary required a few educated guesses as to the proposers' intent. The times quoted above are those from the hardcopies (PDF) versions of the proposals copied from the STScI web site on 28.7.99. These times differ slightly from the output from the NMS Exposure time calculator (copied on the same day). The NMS ETC output currently lists total exposure times of 112, 99, 30, 52, 68 days for the first 5 proposals listed above.

Adding the above proposals up (and leaving item 6 out) gives a total of 363 days, or about 1 year of total exposure time. As mentioned at the start, we will not be making detailed S/N and exposure time calculations in this section. However some general points can be made. With an IFTS, one can efficiently combine the imaging and low spectral resolution parts of all the above proposals. In general in this mode, in the same amount of time, one goes less deep with an IFTS than one would with a single MOS observation, but this is counterbalanced by the facts that (a) one may often want to take multiple MOS exposures of a single region in order to get enough objects (see section 2.5), (b) one may also need to take multiple MOS exposures in order to cover a wide enough wavelength range (a single grating exposure is restricted to at most a factor 2 in wavelength), and (c) for the IFTS one can combine the imaging and spectroscopic time and get both at once. These issues will be addressed in some detail in section 3.

As one moves to higher spectral resolution, and correspondingly looks at less faint objects, the gain from the pure IFTS approach becomes less obvious. Ideally one would use a complementary instrument set with an IFTS for the imaging and faint object low spectral resolution spectroscopy, together with a MOS or IFS for high spectral resolution observations of rarer, brighter objects. An alternative approach, involving the addition of a slit mask and a prism to the IFTS is now a part of the IFTS proposal, and at least at these preliminary stages seems very attractive. In the discussion below, however, we will concentrate on the gains for the lower spectral resolution (R<5000) science.

For the deepest IFTS exposures, one can calculate that there will be of order 10^4 objects with R=100 spectra with S/N>10 within a 5x5 arcminute FOV. For each of these galaxies, an IFTS will deliver diffraction limited, spatially resolved spectroscopy covering the entire galaxy. The basic goal of this document is to list some of the science gains from such data when compared with MOS observations with a few hundred galaxies total and limited to the part of the galaxy sampled by a slit.

We will discuss these science gains under six headings below:

- Evolution of structure
- Location of merging fragments
- Effects of environment
- Spatially resolved star formation histories
- Additional benefits of large galaxy samples
- Other (non-galaxy) DRM goals that can be met with the same IFTS data sets. (see also section 2.4)

2.2.2 Evolution of Structure

The redshift evolution of galaxy clustering is a fundamental test of all theories for the origin of structure in the Universe. There are now a large number of very sophisticated statistical measures for the amount and form of clustering amongst the galaxy population. The simplest of these are the two-point correlation function and the spatial power spectrum. For either of these statistics, samples of a few hundred galaxies along a given redshift column from zero to perhaps as high as 20 will be extremely inadequate.

To illustrate this point graphically, Figure 1 shows a pie diagram from the recently completed CNOC2 survey (Carlberg et al. 1999). The y-axis has been greatly expanded to allow one to see the individual points, but nevertheless one can see that with 1500 galaxies and a redshift column from 0.1 to 0.7 one can begin to see a wealth of structure. Removing 2 out of three points and then spreading those points over an enormously expanded redshift range will make clustering studies impossible. Formal error estimates for the two-point correlation function as a function of number of objects and redshift scale as the square root of the number of galaxies in each redshift bin, and so very large samples are needed.

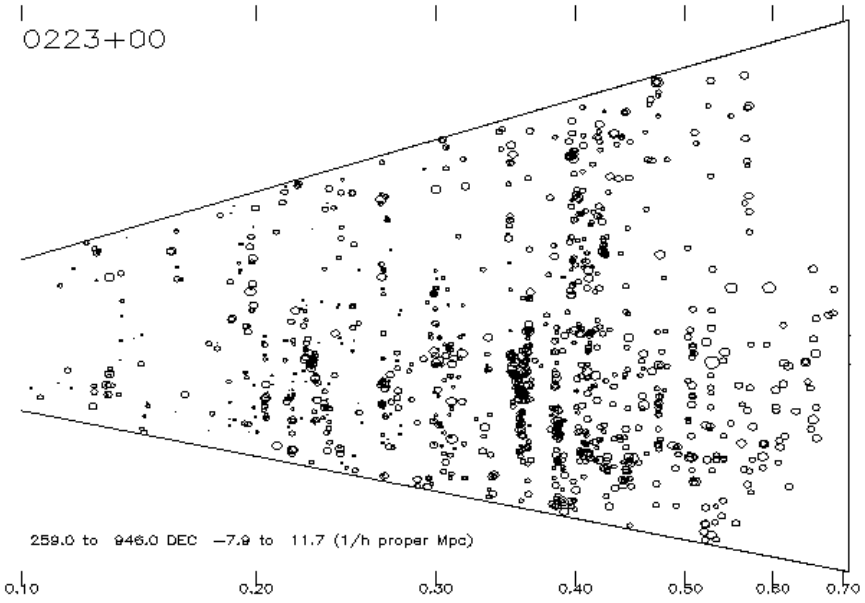

Figure 1: Pie diagram showing ~1500 galaxies in a 2 degree region of the sky surveyed as part of the CNOC2 survey (Carlberg et al. 1999). The x-axis labels are redshift. The tick marks on the y-axis show 1/h proper Mpc

The need for large samples is made more extreme by the clear desire to break up any galaxy sample still further to look for clustering as a function of galaxy properties such as luminosity, colour, star formation rate, or morphology (see Kauffmann et al. 1998). In justifying the request for a sample of 2500 galaxies in order to study evolution in their properties with R=1000 spectroscopy, the GDRM proposes breaking the sample into 5 redshift bins, 6 mass bins and 4 star formation rate bins, yielding 20 galaxies per bin.

Using an IFTS approach to the GDRM will allow us to measure the growth of structure as a function of redshift and galaxy type, an issue central to item 2 on the list of GDRM science goals.

2.2.3 Location of Merging Fragments

Figure 2 shows the results from a HST study by Pascarelle et al (1996). They used a 0.15 micron wide filter to identify objects with Lyman-α emission at z=2.39 associated with a weak radio galaxy. The figure shows 18 candidate 'fragments' spread across a 2.5 arcminute field (corresponding to 0.7 Mpc for h=0.8, q_0=0.5). At least 8 of these fragments have been confirmed spectroscopically, and have been shown to have a relatively small velocity dispersion (~300 km/s). It has therefore been claimed that these fragments will have merged to form an early type galaxy by the present day.

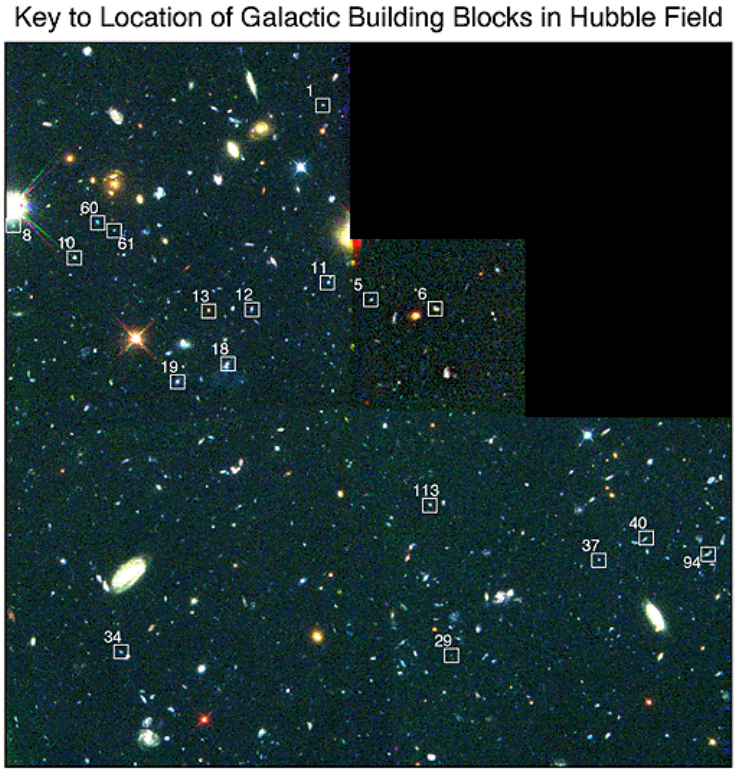

Figure 2: Merging galaxy fragments (Pascarelle et al 1996).

It is clear from Figure 2 that identifying all such fragments over the huge redshift column accessible to NGST, for even a single field, will be extremely arduous without a large set of intermediate width filter observations combined with confirmatory MOS exposures. In contrast, all such fragments will be found in a single IFTS scan. It is true that one would then like to follow up a subset of these fragments at higher spectral resolution in order to measure their velocity dispersion, but a massive amount of winnowing (and initial science) can be done from the basic IFTS observations. This data is also essential for item 2 on the list of GDRM science goals.

2.2.4 Effects of Environment

It has long been known that the morphologies and star formation histories of galaxies are strongly correlated with their environment. Red elliptical galaxies dominate rich clusters of galaxies, while the field contains predominantly blue spirals. More recent work has shown that this correlation is seen even within the 'field' population (Hashimoto et al. 1998). That is, that the star formation and morphologies of galaxies within small groups or generally slightly over-dense regions is also significantly different from that of galaxies in low-density regions. The Hashimoto et al. Study used the LCRS sample of 15,000 galaxies spread over a large angle on the sky, but limited to redshifts less than 0.2. Turning again to Figure 1, it is clear that samples of 100-500 galaxies would not be sufficient to measure the local galaxy density. The IFTS data will produce this additional science (central to item 4 on the list of GDRM science goals).

It should also be noted that the GDRM proposal specifically targeting item 4 in the GDRM science goals (observations of 7 rich galaxy clusters) would also benefit hugely from the IFTS approach. One will instantly be able to separate out cluster members from the field population, and measure their morphologies and star formation rates. One will also be able to identify and obtain redshifts for background-lensed objects

It is also true that item 4 in the GDRM observing plan (looking at regions centred on QSOs) will more or less require an IFTS type of approach. The sorts of galaxies expected to be associated with intervening absorption lines along the line-of-sight to the QSOs are very unpredictable, and only a redshift survey complete to very faint limits can honestly claim to have identified the most likely absorber-galaxy connection.

2.2.5 Spatially resolved Star Formation Histories

Figure 3 shows some very promising attempts to unravel the star formation histories of high redshift galaxies using broad band imaging by Abraham (1998). The key result - that there seems to be coordinated bursts of star formation possibly triggering other bursts at nearby locations within the galaxy is very exciting. It remains true, however, that measuring star formation histories, metallicities and dealing with possible AGN contamination or varying stellar IMFs while using only a few broad band colours is very difficult. Obtaining unique solutions for the above complex sets of parameters is basically impossible.

On the other hand, MOS spectroscopy (putting a single slit across each galaxy) loses almost all of the spatially resolved information that one would like to have to study individual galaxies. Unless one is very lucky, the slit will not lie along the major axis of the galaxy, and even if it does, only a small fraction of galaxies have the convenient chain morphology shown in the two examples below.

For the above reasons, the current GDRM specifically includes IFU observations around 25 galaxies at $z>3$. The IFTS approach will allow us to obtain spatially resolved (3D) spectroscopy at low resolution for all 10^4 galaxies in a deep exposure. No object selection will be necessary and worries about confusion greatly reduced. To expand on this latter point, at the faintest levels it is possible that confusion will be a serious problem. Contaminating fore- and background objects will need to be removed before the fainter sources can be studied. Full 3D information will make such removal possible.

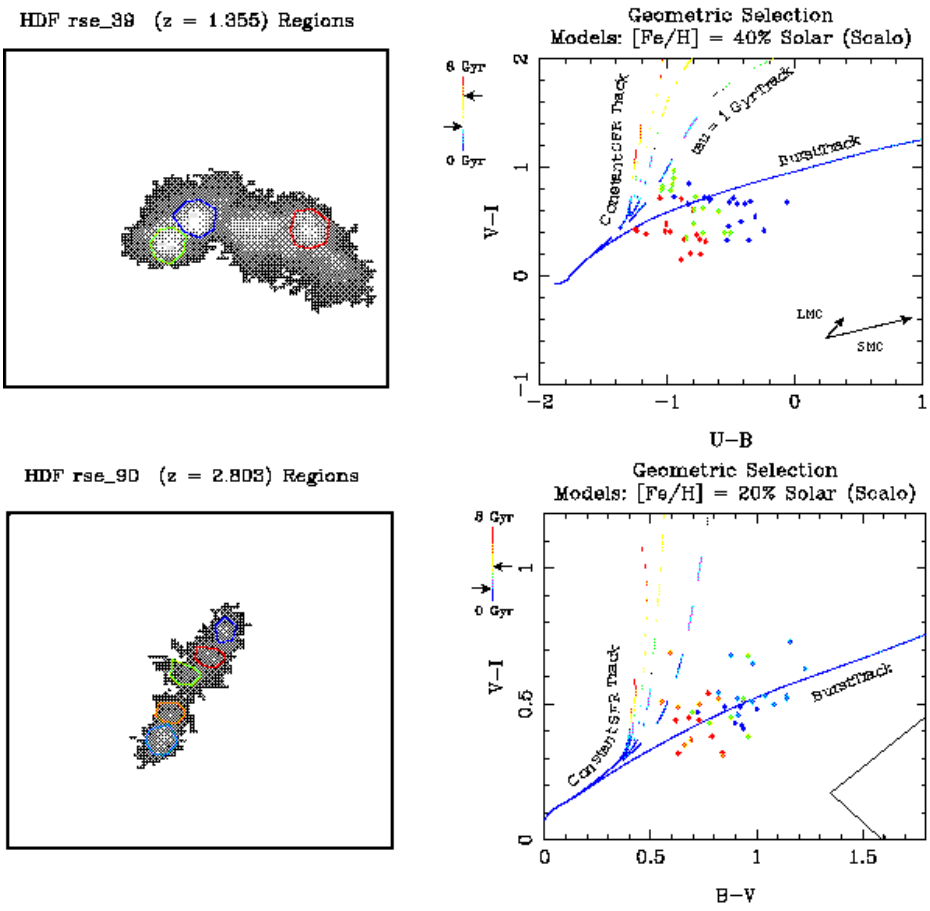

Figure 3: Morphophotometric colour diagrams for two chain galaxies from the HDF. The right hand panels show the distribution of pixel colours within the regions outlined in colour in the left-hand panels. Also shown on the right are models corresponding to constant, exponential and instantaneous star formation. (Abraham 1998).

2.2.6 Additional Benefits of Large Samples to the GDRM

Three rather general points can be made about the benefits of large samples of objects with complete spectroscopic information:

1. Such samples make possible the finding of rare and unusual objects. Some possible examples of such objects would be very high redshift galaxies, Ultra-Luminous InfraRed Galaxies, or low-luminosity, low star-formation rate dwarfs.
2. Another general area needing large samples is anything where one would like to break the galaxy sample into several bins. Immediately obvious cases of this are studies of the star formation rate as a function of redshift, or the evolution in galaxy metallicity with redshift. For both of these one would like to break the galaxy sample into several bins in luminosity, morphological class, and possibly also spectral class. This division (on top of binning in redshift) will rapidly reduce a sample of a few hundred galaxies to statistical meaninglessness.
3. Selection effects often plague studies of galaxy evolution. For once (with an IFTS), spectroscopic selection effects will not be a problem, as no object selection is necessary. One will have spectra of all the objects above a well-defined flux limit.

2.2.7 Other DRM Goals that can be met with the same IFTS data set

DRM projects not in the galaxies section, but which can be addressed using exactly the same data set include:

1. SN searches: during the low resolution IFTS scan, any objects with changing flux can be identified by summing the flux in the two IFTS output ports. Thus Supernovae can be identified even before the completion of a scan. After correction for the varying total flux, a spectrum can be produced from the completed scan. With the spectrum one can identify type Ia SN, and use these standard candles to measure Ω and Λ.
2. Weak lensing: Several parts of the weak lensing proposal in the Cosmology DRM can be done in parallel with the Galaxies observations. Specifically, the requested deep imaging, of random high galactic latitude fields, and also the cluster deep imaging survey.
3. Reionisation and the IGM: Obtaining a high S/N spectrum for high redshift QSOs and hence probing the IGM out to the reionisation epoch will be possible by combining the spectra for all the QSOs in the deep IFTS scans. Such a co-added spectrum would probably be ideal for the DRM program aimed at studying reionisation.
4. Serendipity: although not explicitly listed in the DRM, all astronomers treasure the opportunities for serendipity which come with order of magnitude improvements in capability. The likelihood of serendipitous discoveries based on deep 3D images over a wide field is high. An example of such science is examined in detail in section 2.4.

2.2.8 Summary

In order to address the GDRM science goals, a MOS+Camera combination will require separate imaging, followed by object selection and then a (probably large) number of MOS mask observations in order to build up a large enough sample of galaxies and also to cover each of the different science goals. We have tried to show above that many of the GDRM science goals can be met with a single (or a small number) of IFTS exposures. This will both enable the primary goals of the GDRM, and also add considerable value, permitting considerable science that would not be possible with only the Camera+MOS data. An IFTS on NGST would be a 'serendipity machine' churning out unexpected and exciting results on top of the very important goals of the GDRM.

2.3 IFTS versus MOS S/N Comparison

2.3.1 Context

In this section we try to compare the S/N and data achieved from two different approaches to deep imaging and spectroscopy with NGST. In particular, we will compare what one obtains from observations with a camera+Multi-Object Spectrograph (MOS) combination, with what one can get with an imaging Fourier Transform Spectrograph (IFTS). The total exposure time is held constant for the comparison (~51 days). Within the DRM, very deep imaging and spectroscopy of a single field seems likely to satisfy many of the proposals. The precise proposal we have taken for this comparison is that of Lilly et al., aimed at studying the formation and evolution of galaxies, but this same data can be used for several other DRM goals (e.g. Supernova searches).

A JAVA based IFTS S/N calculator is now available on the web at http://www.hia.nrc.ca/STAFF/slm/ifts.

2.3.2 Assumptions

Limiting fluxes for a given exposure time are calculated using the (somewhat simplified) formalism documented in the mathCAD file 'snr.mcd' (see http://www.hia.nrc.ca/STAFF/slm/ifts). The assumptions built into that calculation are listed in detail inside that file, but include:

- point sources
- 0.05 arcsec pixels (200 arcsec FOV)
- 1 AU orbit
- 1-5 microns, effective M=200, and R=100 (see below)
- for long slit - width 0.23 arcsec

The exposure times in the original proposal for the NIR wavelength range were 28 days for imaging (4 filters, 7 days each), and 23.1 days (2 million seconds) for R=100 spectroscopy over the full 1-5 micron range. We note that it is not detailed in the proposal how a grating or prism spectrograph will deliver this large range in wavelength. Three or more cameras and a combination of dichroics would be needed to cover this full range with gratings or prisms. Alternatively, one could take multiple exposures with different wavelength coverage at the cost of going less deep. For the comparison below, we consider three different possibilities:

1. That the MOS can get the full 1-5 micron range onto some detector or combination of detectors at the same time. (I.e. prisms or at least three dichroics).
2. That the wavelength range observed is limited to just the range 1-4 microns, and:
   - The MOS can observe this full range at one time (i.e. prisms or at least 1 dichroic), or
   - The MOS has to take 2 exposures to cover 1-2 microns and then 2-4 microns.

There are other exposures listed in the Lilly et al. proposal to cover the optical and thermal IR, and also higher resolution spectroscopy, but for this comparison, we will stick to just the 1-5 micron part of the science.

2.3.3 Spectral Coverage and Resolution

It is probably worth emphasising here that an IFTS with a single beamsplitter can in principle cover an extremely wide wavelength range. The beamsplitter efficiency can be shown to remain high (reflectivity times transmission times four greater than 0.8) over a wavelength range of a factor 7, in contrast with the usual factor of 2 of a grating.

The spectral resolution of both a dispersive spectrograph and also an IFTS varies with wavelength. For dispersive spectrographs, the resolution is proportional to the wavelength. For an IFTS it is proportional to one over the wavelength. As a result, one can only match the resolution of the two systems at one wavelength. For this comparison, we have basically chosen to divide the 1-5 micron range into 200 evenly spaced samples in both cases (in wavelength for dispersive, in frequency for the IFTS), and assume that the spectral resolution will be roughly critically sampled.

For most applications, having higher spectral resolution at the shorter wavelengths (i.e. the IFTS situation) seems a better match to the scientific requirements. At the red end of the 1-5 micron range, the background is higher, and the photon rate from many classes of astronomical objects is lower.

2.3.4 Results

Using the above estimator, one can calculate that the above exposure times will yield the following flux limits for the Camera+MOS combination:

2.3.4.1 1-5 microns, MOS with 2 or more dichroics

Table 1: Camera+MOS flux limits, 2 or more dichroics

Wavelength	1-2 microns	2-3 microns	3-4 microns	4-5 microns
5σ Imaging, AB	34.8	34.3	33.7	32.6
5σ Imaging, nJy	0.04	0.07	0.12	0.34
10σ Spectro, AB	31.6	30.8	30.3	29.9
10σ Spectro, nJy	0.82	1.7	2.8	4.5

Obviously, one could trade time between different filters, and between imaging and spectroscopy to balance out the flux limits more if desired.

Designing an equivalent IFTS observation involves similar choices. Below we tabulate the flux limits in spectroscopy and broad band, assuming one has chosen to observe with the same 4 filters as used for the camera observations above, but that while doing this one also scans through 50 IFTS spectral channels. When the resulting 4 exposures are combined one will end up with a spectrum with 200 spectral channels running from 1-5 microns. We also have weighted the exposure times to give rather more uniform S/N as a function of wavelength, while keeping the total exposure time roughly equal to that assumed for the Camera+MOS combination. If anything this weighting makes the IFTS option look worse, as one has to spend a lot of time at 4-5 microns to get matching S/N to the 1-2 micron region.

Table 2: IFTS flux limits, 1-5 micron scanned

Wavelength	1-2 microns	2-3 microns	3-4 microns	4-5 microns
Exposure time	5.8 days	8.7 days	14.5 days	23.1 days
5σ Imaging, AB	34.7	34.4	34.1	33.2
5σ Imaging, nJy	0.05	0.07	0.08	0.19
10σ Spectro, AB	29.4	29.3	29.0	28.2
10σ Spectro, nJy	6.1	7.9	9.2	19.4

2.3.4.2 1-4 microns, MOS with 1 or more dichroics

For this comparison, we have backed away from observing the full 1-5 micron range. This means that a dispersive spectrograph with gratings or prisms can cover the entire range in principle with only one dichroic. This also helps the IFTS, in that the time needed to get reasonable S/N in the 4-5 micron wavelength range for the IFTS is large. We have kept the total exposure time the same as above, and hence go deeper in both cases; the difference in depth is (unsurprisingly) smaller.

Table 3: Camera+MOS flux limits, 1 or more dichroics

Wavelength	1-2 microns	2-3 microns	3-4 microns
Exposure time, days	9.3	9.3	9.3
5σ Imaging, AB	35	34.4	33.9
5σ Imaging, nJy	0.04	0.06	0.1
Exposure time, days	23	0	0
10σ Spectro, AB	31.6	30.8	30.3
10σ Spectro, nJy	0.82	1.7	2.8

Table 4: IFTS flux limits, 1-4 microns scanned

Wavelength	1-2 microns	2-3 microns	3-4 microns
Exposure time, days	11.6	17.4	23.1
5σ Imaging, AB	35.1	34.8	34.4
5σ Imaging, nJy	0.03	0.05	0.06
10σ Spectro, AB	29.9	29.6	29.3
10σ Spectro, nJy	4	5.3	7.1

2.3.4.3 1-4 microns, MOS with no dichroics

Finally we show the Camera+MOS sensitivities in the case where one has to take two spectroscopic exposures. This further reduces the difference in depth between the IFTS (table 4 above), and the dispersive system.

Table 5: Camera+MOS flux limits, no dichroics (i.e. 2 exposures with spectrograph)

Wavelength	1-2 microns	2-3 microns	3-4 microns
Exposure time, days	9.3	9.3	9.3
5σ Imaging, AB	35	34.4	33.9
5σ Imaging, nJy	0.04	0.06	0.1
Exposure time, days	8.1	15	0
10σ Spectro, AB	31.3	30.6	30
10σ Spectro, nJy	1.1	2.1	3.5

2.3.5 Discussion

Unsurprisingly, given that one is effectively exposing for twice as long total in imaging, one can go fainter in broad band with the IFTS approach at most wavelengths (although the varying exposure times makes this difference a function of wavelength). Conversely, one gets significantly less deep in spectroscopy. This penalty essentially arises, as, even with NGST, at these flux levels, one is background limited. Lower dispersion, or brighter flux levels (i.e. shorter exposure times) would make the IFTS flux limits closer to those of the MOS. If one were driven to making multiple exposures with the MOS in order to cover the full 1-5 micron range, some of the MOS depth advantage would obviously be lost.

2.3.6 Object density and morphology

What is not contained in the above tables is the number of objects one will have usable spectra for at the end of the experiment. An additional issue is the capability with the IFTS data to tune the aperture over which one sums up the spectrum to match the morphology of the object. This latter capability – delivering spatially resolved spectra for galaxies – is a large qualitative advantage over the multi-slit approach. However, putting this aside, let us consider the number counts at these faint levels. The NICMOS HDF observations summarized by Thompson et al. (astro-ph/9810285) show that at AB(1.65 microns)=29, there are between 100 and 200 objects per square arcminute per magnitude. For the assumed 317 arcsec FOV of the IFTS, and assuming one is interested in objects with a range of at least 3-4 magnitudes, one ends up with 8000-20000 objects in the above IFTS

exposure for which one will obtain spatially resolved spectra with S/N in the continuum greater than 10.

For the MOS observation, one can clearly go fainter, indeed one could obtain spectra for objects a magnitude fainter than are visible in the current NICMOS HDF image. However, one will have to choose around 100 of these to observe. (The latter number is somewhat picked from thin air. We would be interested in realistic estimates of the number of objects one can put slits on with proposed MOS+camera combinations.) An alternative way of looking at the issue is given in section 2.5. One could choose to obtain multiple MOS exposures to get the number of objects up, at the cost again of going less deep, but it would be impractical to observe anything close to the possible 20000 objects measured in the IFTS exposure.

An issue we will not address here is whether all 8000-20000 objects in the IFTS data are really of scientific interest. Clearly the MOS targets can be chosen to focus in on a particular, high-priority science goal. However, we suspect that a very large fraction of the objects with IFTS spectra will be of interest for some NGST science, and even if not, it may be necessary to have data on them to help deal with crowding and confusion of the primary science targets.

As an aside, we reiterate here that the IFTS data can be used for supernova searches, while any equivalent MOS observations have no such opportunity for serendipity.

2.4 Bonus Halo Science from IFTS approach to the GDRM

2.4.1 Introduction

An IFTS onboard the NGST would broaden the scientific impact of the data taken for the GDRM, increasing the productivity and potential of the telescope. The fact that every single object in the IFTS-observed GDRM fields will have simultaneous imaging and spectroscopy means that there could be a significant number of halo objects with potentially useful images and spectra available for analysis (there is also, of course, the potential for unpredicted populations of objects in the GDRM fields, further increasing the impact of the IFTS and NGST). If the number of halo objects is significant, then these serendipitous observations could have an appreciable scientific impact (which would be completely unrealised with a camera+MOS). It is the purpose of this section to estimate the stellar contribution of (or contamination of, depending on your point of view) the data-cubes obtained for the GDRM.

2.4.2 Halo Stars in the GDRM

Since the GDRM fields are nominally located at high galactic latitudes, the Galactic component that will provide most of the stellar contribution is the Galactic halo. The halo itself is composed of the standard Galactic stellar spheroid, with a local mass density of $\sim 2.4 \times 10^{-5} M_{Sun} pc^{-3}$ (Graff & Freese, 1996a), and a dark component (composed of e.g. brown dwarfs, white dwarfs, unknown dark matter), with a local mass density of $\sim 7.9 \times 10^{-3}$ $M_{Sun} pc^{-3}$ (assuming the standard MACHO model, Alcock et al 1997). The contribution to the GDRM fields from the stellar spheroid component can be estimated easily enough using a Galaxy Model (e.g. Bahcall & Soneira, 1981), but the contribution from the dark component is obviously dependent upon the nature of the matter making up this component (i.e. can it be observed if one looks hard enough?).

Results from recent microlensing experiments (Alcock et al. 1997) have shown that the halo mass in the form of MACHOs (Massive Collapsed Halo Objects) is in the range (1.3-3.2) x1011MSun --- the total mass in the halo is $4.1x10^{11}M_{Sun}$. Although this estimate of the mass in MACHOs is fairly independent of the model chosen for the halo, the average mass of the MACHOs is highly model dependent. Alcock et al. find that the most probable average mass for the lensing objects is ~$0.5M_{Sun}$, with the likely range extending from (0.05-1.0) MSun. If these estimates are correct, then roughly half of the mass of the dark halo of the Galaxy is in the form of ~$0.5M_{Sun}$ objects: since the mass function of white dwarfs (WDs) is strongly peaked around $0.6M_{Sun}$(Koester et al., 1979), and old WDs are intrinsically faint, they provide an obvious candidate for the MACHOs.

The visibility of WDs to the NGST is highly dependent upon their cooling rate, which is itself highly dependent upon the composition of the WD's atmosphere. While early models of cooling WDs were essentially blackbodies, and so followed an easily predictable path in a colour-magnitude diagram (CMD), recent models with more realistic atmospheres (Hansen 1998, Saumon & Jacobson 1999) have shown that this is not necessarily the case. At temperatures less than ~4000K, hydrogen molecules (H2) will begin to form in a WD's atmosphere, producing a broad band of absorption at wavelengths longer than ~1 micron: this suppresses the continuum flux at long wavelengths but, due to re-emission of the absorbed radiation, produces an enhanced continuum flux at shorter wavelengths. The effect of this H2 absorption is to cause WDs, as they cool below 4000K, to become bluer, deviating from the classic blackbody-cooling curve. For WDs with helium-rich atmospheres, the lower opacity of neutral helium will allow these stars to cool much more rapidly than their hydrogen-rich counterparts, and will cause them to cool approximately as blackbodies (i.e. they will become redder as they cool). Due to their more rapid cooling, helium-rich WDs will be much fainter than hydrogen-rich WDs at the same age, even at infrared wavelengths: hence, the contribution from WDs in the halo to the stellar content of deep NGST images will be dominated by hydrogen-rich WDs. On the other hand, the fraction of WDs with a hydrogen-rich atmosphere is expected to be less than 100% for any progenitor population; however, since the mechanisms which produce WDs with a helium rich atmosphere (primarily convection) are expected to become efficient at moderately high metallicities, it is probably safe to assume that 50% of the WDs in the metal-poor halo have hydrogen-rich atmospheres (Hansen, 1999).

From the infrared colours of hydrogen-rich WDs (provided by Saumon 1999, private communication), and the fact that such a WD will have a temperature of ~3500K at ~10^{10} years (Hansen, 1999), we can expect WDs in the halo to have an absolute K magnitude of M_K~16. At limiting magnitudes of K~34 and K~31 for the deep and shallow NGST fields, these WDs should be detectable out to ~40kpc and 10kpc, in the respective fields. Using the MACHO model for the Galaxy halo, which has a density distribution of:

$$\rho_H(r) = \rho_0 \frac{R_0^{\,2} + a^2}{r^2 + a^2}$$

[where $\rho_0=7.9x10^{-3}$ $M_{Sun}pc^{-3}$ (the local dark matter density), R_0=8.5kpc (the distance of the Sun from the center of the Galaxy), a=5kpc (the halo scale length), and r is the distance from the center of the Galaxy], the enclosed mass in each of the observed 5'x5' fields should be:

	Limit Mag	Enclosed Mass (Msun)	Expected # of WD
Deep Field	34	7200	3000
Shallow Field	31	550	230

Given the expected halo mass composed of WDs (assuming they are the MACHOs), the expected number of observed WDs can be found simply by dividing the above masses by the average mass of a WD (~0.6MSun). However, given that only ~50% of the halo is potentially made of WDs, and that only ~50% of the WDs in the halo are of the hydrogen-rich variety, only ~25% of the mass enclosed in the survey fields will be composed of observable WDs. Nonetheless, the expected numbers of WDs in the GDRM fields are huge: ~3000 in the deep field and ~230 in each of the shallow fields (~3600 total from the sixteen shallow fields). Even if WDs comprise only 10% of the halo mass, rather than 50%, or if the limiting magnitudes of the fields are brighter by one or two magnitudes, there will still be a significant number of WDs observed in the GDRM fields. Re-doing the above estimates for the HDFN yields ~2 WDs expected down to V~28, consistent with the observed number of stellar objects in the HDFN at the appropriate colours (~0, depending on the age of the halo; Hansen, 1998). A recent pre-print from Ibata et al. (1999) shows that two blue stellar objects in the HDFN have high proper motions relative to the background of galaxies: their high rate of motion supports the hypothesis that they are local halo objects, and their blue colours suggest that they are, in fact, the hydrogen-rich WDs which have been predicted. If this is the case, the numbers of predicted WDs in the GDRM fields are likely to be reasonable.

The expected number of normal halo stars can be found in a similar manner to that used for halo WDs. Assuming a mass function which turns over from a slope of x=2.35 to a slope of x=1 (dN/dm proportional to m-x) at a mass of $0.2M_{Sun}$, roughly 270 stars per NGST field should be observed (the numbers should be roughly the same in both the deep and shallow GDRM fields since it is the truncation of the halo, assumed to be at 50kpc, rather than the luminosity of the faintest stars, which sets the limit to the number of stars observed).

Despite the fact that the fraction of the halo contained in brown dwarfs may be as high as 3% (Graff & Freese, 1996a), there should be few, if any, observed in the GDRM fields. Extrapolating the results of Burrows et al. (1997), the expected K-band luminosity of $\sim 0.04M_{Sun}$ brown dwarfs should be fainter than M_K~23. The deepest GDRM field should contain no more than $\sim 0.10M_{Sun}$ in halo brown dwarfs, which translates in to an expected number of ~3 brown dwarfs.

2.4.3 Scientific Impact

The GDRM observations will yield, as a bonus, images and low resolution (R~100) spectra for potentially thousands of WDs in the Galactic halo. The number of WDs actually observed will allow us to:

1. Place stronger limits on the mass of the Galactic halo contained in WDs.
2. Determine the age of the Galactic halo to high confidence.
3. Refine the estimates of the optical depth due to WDs, which will affect the interpretation of the MACHO results.

The GDRM is one of the primary science drivers for the NGST. Using a true imaging spectrometer, such as an IFTS, to obtain the GDRM observations further increases the impact of the programme by allowing other science projects to be carried out using the same data. As outlined here, the GDRM observations will contain thousands of WDs, providing enough information to discern whether faint WDs can account for most of the dark matter in our own Galaxy. Constraints on this WD population will allow us to further understand the formation of the Galaxy and its stellar populations, which will in turn broaden our understanding of galaxy formation and evolution in general. Potentially, such constraints on the baryonic dark matter content of galaxies could affect the

interpretation of the GDRM galaxy data: without the contribution of an IFTS onboard the NGST, this complementary feedback would be unrealised.

The halo WD observations within the GDRM data are just one example of the additional scientific data that will be obtained with the IFTS. Observation of such populations of objects are not, in fact, truly serendipitous, such as observations of supernovae in the GDRM fields will be, since we know that such a population will be present in the data. The full potential of the NGST IFTS data can only be grasped if there is a full understanding of the populations, both near and far, which will be present in the fields being studied --- without an IFTS this potential will be only partially achieved, without the expense of additional observing time.

2.5 IFTS/MOS Comparison (contributed by James Graham)

Several DRM programs call for low resolution spectra of large numbers of faint (K >29 AB) objects. Since dispersive spectrometers on NGST are dark current limited, they are unsuitable for surveys that require observations of large samples. This survey science is crucial to NGST, for example, one component of the galaxy evolution DRM consists of validating photometric redshifts with R~100 spectroscopy. The accuracy and precision of photometric redshifts should be investigated over a range of galaxy properties. Since statistical errors scale as the square root of the number of galaxies in each bin, of order of 100 galaxies are needed per bin. Without such large numbers, multiplicative factors decimate small samples to statistical meaninglessness. A modest sample to test photometric redshifts consists of 10-redshift x 5-luminosity x 2-color x 3-environment x 3-morphology bins x 100 galaxies per bin = 90,000 galaxies. The FTS can perform a complete magnitude limited sample to K=29 AB in three days. A MOS would take 45 days to complete this survey.

To discover and characterize the population of sources which re-ionize the universe at z >~ 10 requires winnowing out sources which comprise <0.1% of the population at K~29-30 AB (Haiman & Loeb 1998). Clearly thousands of spectra are needed for this task to: 1) find the high-z population; 2) distinguish AGN from objects powered by star formation. Once these distant star-clusters, galaxies, or quasars have been identified, their spectra may be coadded to construct a very high signal-to-noise ratio composite spectrum that is a sensitive probe of the re-ionization epoch. Rather than hoping to find a single bright target in the dark ages, composite spectra may be the most reliable way to search for the re-ionization epoch: the luminosities and masses of the first collapsed objects are unknown, and there are likely to be many more small (faint) ones than large (bright) ones.

These observations suggest that it is appropriate to define the figure of merit used to compare a MOS and an IFTS as the ratio of the number of galaxy spectra obtained. We assume that a magnitude-limited catalogue is obtained in a fixed observing time, and the same wavelength range and number of spectral channels for each instrument.

For a single object under photon shot noise limited performance a dispersive spectrometer is faster than the IFTS by a factor which is proportional to R. Thus if the integral number counts scale as $\text{flux}^{-\alpha}$, then the speed of the IFTS compared to a MOS is proportional to $f_0^{-\alpha}/(N_{slit}\ R)$ where f_0 corresponds to the magnitude limit of the catalogue. N_{slit} is the number of MOS slits (assuming one object per slit) and R is the spectral resolution. Since the predicted value of alpha is about 1, the conclusion is that at faint enough flux level the IFTS always wins. The conclusion is stronger than this because dispersive spectrometers on NGST are dark current limited. Dispersive spectrometers are only photon shot

noise limited for bright (K < 26 AB) objects. Therefore, for targets fainter than this the MOS enters the domain of diminishing returns.

Consider the following more realistic comparison adopting the following set of parameters for the IFTS and the MOS

IFTS FOV = 5' x 5'
N_{slit} of the MOS = 1000
Spectral resolution = 100
wavelength range = 1.3 - 2.6 micron (i.e. the FSR of a m=1 grating blazed at 2 microns)
idark = 0.02 electrons per second
rnoise = 4.0 e- rms read noise
tmax = 800.0 sec maximum time before readout to veto cosmic rays

The objective is to observe as many galaxies as possible with fluxes greater than or equal to a given magnitude limit. The IFTS observation is conducted by using the entire integration time to observe one field. For bright objects, the MOS has the speed to observe multiple fields. Thus the number of MOS spectra equals N_{slit} times the number of pointings. The surface density of galaxies is derived from the Haiman and Loeb (1998) and Im & Stockman simulations and normalized to deep NICMOS counts. The total number of galaxies with spectra with SNR > 10 are plotted on the y-axis of the figure below. The two plots that make up the figure 4 below are two projections of a single 2-d surface that describes the results of the observation. Either the total observation time, or the limiting magnitude of the survey, can be considered as the independent variable.

For K < 26 AB, the MOS is photon shot noise limited, and in a given exposure time is a fixed factor faster than the IFTS. The MOS can take data for ~ 10 pointings and obtain spectra for ~ 10,000 bright galaxies. Because such bright galaxies are rare the IFTS can only obtain spectra for a few thousand galaxies within its field of view. However, beyond K > 26 AB the MOS performance is limited by dark current, and the speed advantage relative to the IFTS declines. Thus by K = 26.9 AB the MOS and the IFTS acquire equal numbers of galaxies. As we enter the domain of scientific interest to NGST, K > 28 AB, the IFTS obtains an order of magnitude more galaxy spectra than the MOS.

Inspection of figure 4 below shows that the only practical way to complete the two examples of low R spectroscopy from the DRM is with an IFTS.

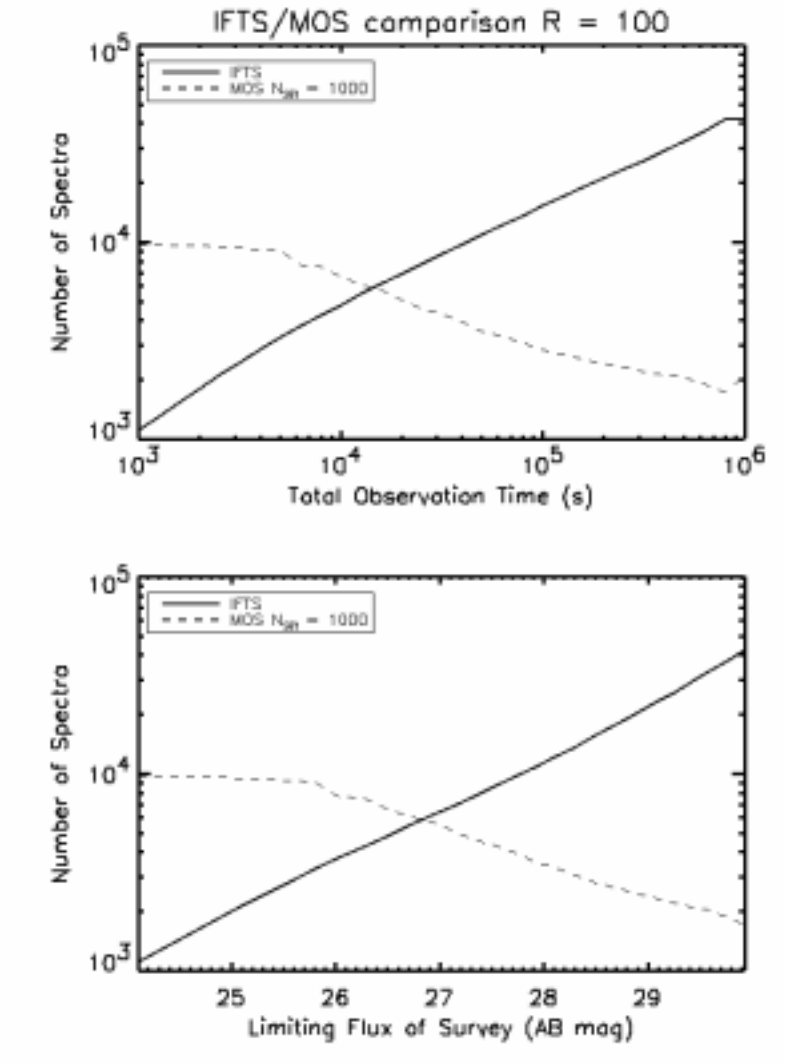

Figure 4: Comparison of the number of galaxy spectra acquired by imaging Fourier Transform Spectrometers and Multi-Object Spectrographs.

3. Engineering

3.1 Introduction

In section 3.2 we present an overview of the concept of the instrument as well as the trade studies, performances and risk analyses that were performed to arrive at the design. In Section 3.3 we address the question of technological readiness. Finally in Section 3.4, we present the breadboarding activities centred on the design and fabrication of a working ground demonstrator aimed at testing the key risk factors identified in the risk analysis.

3.2 Design Concept

3.2.1 Overview

In its most basic expression, a Fourier transform spectrometer is a Michelson-like interferometer. The entrance port of the interferometer is directed at an object and one of the two mirrors is displaced so as to change the optical path difference between the two beams of the interferometer. The motion of the mirror modifies the interference pattern recorded by a detector at the output port of the instrument. The changing interference pattern recorded by the detector forms the *interferogram*. This interferogram is then Fourier transformed into the spectra of the observed object. The spectra can then be calibrated in absolute radiometric units after the radiometric gain and offset of the instrument have been determined. An imaging Fourier transform spectrometer uses a focal plane array of detectors rather than a single detector element. An image of the field is formed on the detector array, so each pixel receives the corresponding interferogram.

Even if FTS are a mature technology and have been flown successfully onboard space platforms (see section 3.2) as well as being extensively used onboard aircraft, balloons and ground based vehicles, the requirements of NGST are somewhat outside of the traditional range of operation of FTS, so that the specific design must be chosen with care. For instance, the very low photon fluxes from the faint targets of NGST will require unusually long exposure times. This constraint implies that the IFTS onboard NGST will be used in a new regime of time scales, see Figure 5. The factors affecting the stability (thermal, mechanical and radiometric) do not have the usual weight. The FTS trade space is well known at Bomem, and the NGST instrument conception could benefit substantially from Bomem’s experience to achieve a design that is optimal.

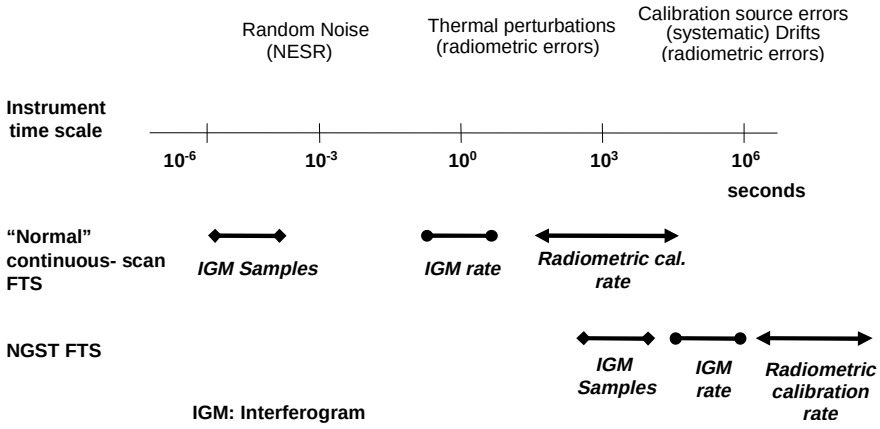

Figure 5: This figure compares the time scales of "normal" or commercial FTS instruments with those for NGST. interferogram data points are acquired in the audio range and interferograms are obtained at a rate of a few per second or one every few seconds. Above the time scale are shown typical perturbations affecting the instruments. On the other hand, the radiant fluxes for NGST are so weak that very long detector exposures are required at each interferogram samples. The best method to achieve the operation at each optical path difference (OPD) is to step-and-stare, using the so-called step-scan method. The time period for which the mirrors must be held at fixed OPD is much longer than any commercial instruments. In particular, the accuracy with which the interferometer can hold the OPD is a crucial parameter (see next panel on right).

3.2.2 IFTS Trade Studies

The goal of our trade studies was to elect the best technological approaches and concepts for the NGST IFTS. Several design options were considered, evaluated and ranked according to their suitability for NGST. Following is a summary of these analyses. Details can be found in RD 20 (in Appendix B.3). It is important to note that a bias towards the most capable, but inevitably more expensive solution was applied so as to produce a somewhat pessimistic estimate of cost and complexity, that could be descoped at will.

Although the final spectral range of NGST has not been decided yet, it is probable that a single detector type will not be sufficient to cover the whole spectral range (the core range is from 1 to 5 μm the extended range is potentially from 0.6 to 30 μm). This implies that the signal must be spectrally separated and directed to the appropriate detector. Several *spectral separation* options were considered. The spectral separation can be performed in front of or after the interferometer. Scanning mirrors, pupil or field dissectors, dichroic splitters can be used. Each method has its advantages and drawbacks. The analysis showed that using dichroic splitters in front of the interferometers resulted in the highest performance and best image quality. This option is more costly as it necessitates one interferometer per spectral band and would likely have dedicated condensing optics (a volume and cost driver) for each interferometer module.

A Fourier transform spectrometer acquires interferograms of the target. These interferograms are produced by the displacement of a mirror in an interferometer. There are different ways of displacing that mirror. The mirror can be displaced step-by-step: the mirror is translated to a new position, stopped during the acquisition of data and moved again to a new position. The motion can be continuous but very slow so as to acquire a single interferogram during the total exposure time. The motion can also be continuous at a higher velocity such that *n* interferograms are acquired during the

total exposure time and then coadded to increase the signal to noise ratio. These three options were analyzed considering available actuators, duty cycle efficiency, position accuracy, power consumption, modulation efficiency, sensitivity to cosmic rays, etc. The selected option is the step-scan. When there is a choice, step-scanning is not usually the preferred sweeping method because of increased stability requirements to reach the sensitivity. These stability concerns remain at the heart of the design of the NGST IFTS.

A FTS works by collecting samples at well known optical path differences. The traditional method to measure the optical path difference (OPD) is to inject a metrology laser beam in the optical path. The interference pattern of the metrology signal is used to continuously monitor the OPD. One potential problem with this technique is to have the metrology light reach and saturate the science detectors. To separate the laser light from the science light, several options are possible. The laser light can be spatially separated from the science light for example by segregating the metrology and science light using baffles or simply a separate interferometer with its moving mirror installed on the main sweeping mechanism. The wavelength of the laser can also be chosen outside the spectral band of the science detector. In the case of a step-scan interferometer, an interesting possibility also exists. The metrology laser can be turned off when the detector is measuring the target. Alternatively, monitoring of the mechanical motion of the moving mirror is possible using, for example, a capacitive sensor. Considering the attenuation factors required to not affect the faint targets of NGST and the accuracy required on the position and alignment of the moving mirror, the selected option is the temporal separation of the metrology.

The metrology method used to control the mirror motion is described in RD 6 (Appendix A.5). In summary, the interference pattern of a laser beam injected in the optical path is monitored by a set of detectors. The number of detector elements per array does not need to be large; eight is sufficient. These arrays are used to monitor the motion of the fringes and their orientation. This information is used to determine the position of the moving mirror and to control the linear actuator that moves the mirror. It is also used by the servo-loop that commands two piezoelectric actuators that correct the alignment by tilting the fixed mirror. Once the moving mirror has reached the desired location, it is clamped in position. The alignment is then corrected by the servo-loop, if necessary.

Other trade studies considered the use of flat mirrors vs. corner reflectors for the mirrors of the interferometer and the number of output ports of the design. The option that results in the highest transmission efficiency is a system with flat mirrors and two output ports. A two-output port flat-mirror Michelson interferometer is possible by injecting light off the optical axis (see Figure 6).

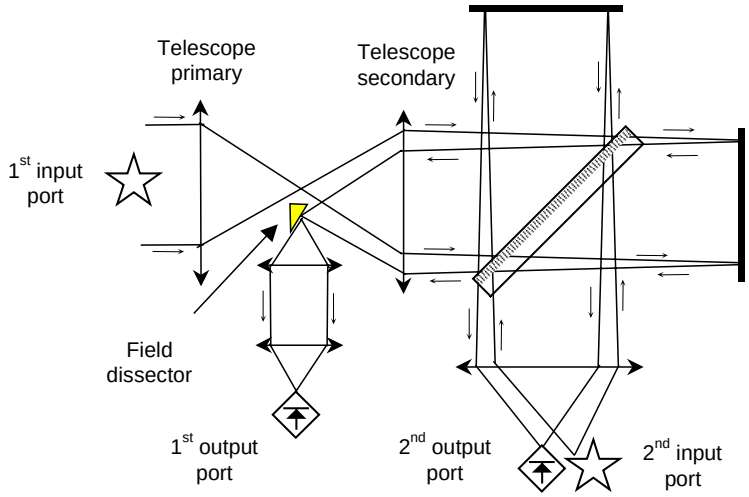

Figure 6 : A two-output port Michelson interferometer using flat mirrors.

In order to measure absolute radiometric quantities, any instrument must be properly calibrated. Fourier-transform spectrometers only require two measurements to fully calibrate the instrument if the detectors are linear (RD 25). Calibration can be performed on the ground prior to launch. It can also be performed inflight using stellar references or onboard calibration sources. Inflight calibration using onboard calibration sources provides the most accurate calibration method although it requires dedicated hardware. Onboard calibration sources need to be high emissivity blackbodies. The traditional method is to operate one source at a relatively cold temperature and another at a relatively warm temperature, so as to cover the expected range of radiance for all wavelengths. Commercial Fourier transforms spectrometers with internal calibration sources routinely achieved high radiometric accuracy and repeatability. Calibrated radiance collected during a field campaign in 1997 by the University of Wisconsin, with two different instruments, each equipped with its own calibration system, differed by only 0.8% over a wide spectral range, see Appendix A.2.

3.2.3 Instrument concepts

The results of the combined trade analysis suggest that the optimal design would be a system that

- Spectrally separates the signal at the entrance using dichroic splitters (if more than one spectral range is used). Each band is then directed to its own IFTS.
- Uses a step-scan moving mirror. A step-scanning mirror is attached to a sweep mechanism and displaced with a precision linear actuator. The mirror is moved to its acquisition position then held in position while the signal is acquired. The process is then repeated a number of times that is determined by the chosen spectral resolution.
- The OPD and interferometric alignment is monitored and realigned during OPD transitions. When the science signal is being acquired, the metrology is turned off to avoid any light contamination.
- Has two output ports. Having two output ports increases the efficiency by a factor $\sqrt{2}$. However such an approach also requires twice the number of detectors arrays compared to a single port system. If this approach is too costly, the system can easily be changed to a single port instrument.

- Uses flat mirrors rather than corner reflectors to reduce the number of reflective surfaces and minimise modulation loss due internal trihedral errors.
- Uses auto alignment based on the sensing of the metrology wavefront errors and effecting correction using two actuators.
- Has an onboard calibration system to perform periodic inflight radiometric calibration. Such a system relies on high-precision blackbodies to correct potential changes of spectral response and transmittance.

Figure 7 shows the interferometer and its subsystems. The calibration sub-system is not shown. The spectral range of such an IFTS system will mainly be limited by the spectral response of the available detectors and the chosen beamsplitter. With the appropriate suite of detectors, an IFTS can easily measure spectra from the ultraviolet to the thermal infrared. No beamsplitter coating can cover a band as large as 0.3 to 30 μm, but such a broad coverage can be obtained by using a small number of beamsplitters. Considering the current capabilities of coating manufacturers, it is reasonable to believe that a single beamsplitter (see Graham et al, 1999) per detector type (one for 0.6-5.6 μm and one for 3-28 μm) will be adequate.

The spectral resolution is also adjustable because it is determined by the maximum OPD in a sweep, which is freely adjustable up to the maximum mechanical displacement. In parallel to the mechanical limit, depending on the optical design the spectral resolution may be limited by the divergence of the light travelling in the interferometer towards a single pixel. Values over R=10,000 can easily be achieved in a spectral band between λ=1 μm and 5 μm for the proposed NGST design. Of course, for the faintest targets, broader spectral resolution settings will be used in order to increase the signal to noise ratio.

Some of these options, e.g. the step-scan mechanism and temporally separated metrology, carry a certain level of risk and thus call for a mitigation plan. This is the object of Sections 3.2.5 and 3.4. The performance of the NGST IFTS are presented in the Section 3.2.4.

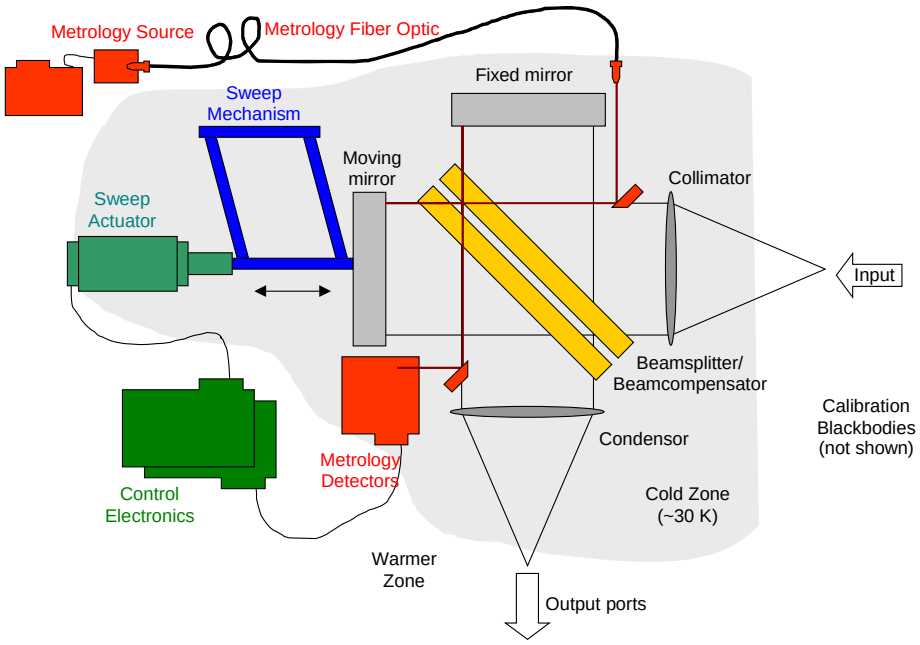

Figure 7 : The interferometer and its subsystems.

3.2.4 Performance Analyses

Performance analyses were carried out to determine if the FTS approach would satisfy the NGST SNR requirements. They were also performed to determine the required accuracy on the position of the moving mirror. The analysis guided the choice of the actuator selected to translate the mirror.

The signal to noise ratio was computed for various values of OPD errors. The results are displayed on Figure 8. The photon noise, the readout noise, the dark noise and the noise caused by positioning errors were considered in the analysis. The zodiacal light was considered in the input signal. Table 6 gives the main input parameters used in the simulation. Details of this analysis can be found in RD 21 (Appendix A.4). Other performance analysis were performed such as signal to noise ratio vs. resolution factor (R), signal to noise ratio vs. magnitude of target, etc. They can be found in RD 21 as well.

The results displayed on Figure 8 indicates that a position accuracy of 1% or better will have a negligible effect on the signal to noise ratio of faint targets. For brighter targets, the effect is more important but the signal to noise ratio for these targets is much higher (see RD 21 for details).

Table 6 : Input parameters for simulation of signal to noise ratio

Parameter	Value
Primary Telescope diameter	8 m
Pixel FOV	0.0387"
Orbital distance	1 AU
Mean Temperature of instrument	50 K
Read-out noise	5 e
Dark current	0.03 e/s
Transmission efficiency	0.83
Modulation efficiency	0.90
Quantum efficiency	0.95
Max. wavelength	5 µm
Min. wavelength	1 µm
Number of spectral bins (R)	100
Exposure time	$1x10^5$ s
Apparent magnitude of target	31.4
Temperature of BB target	5700 K
Red-shift of target	5

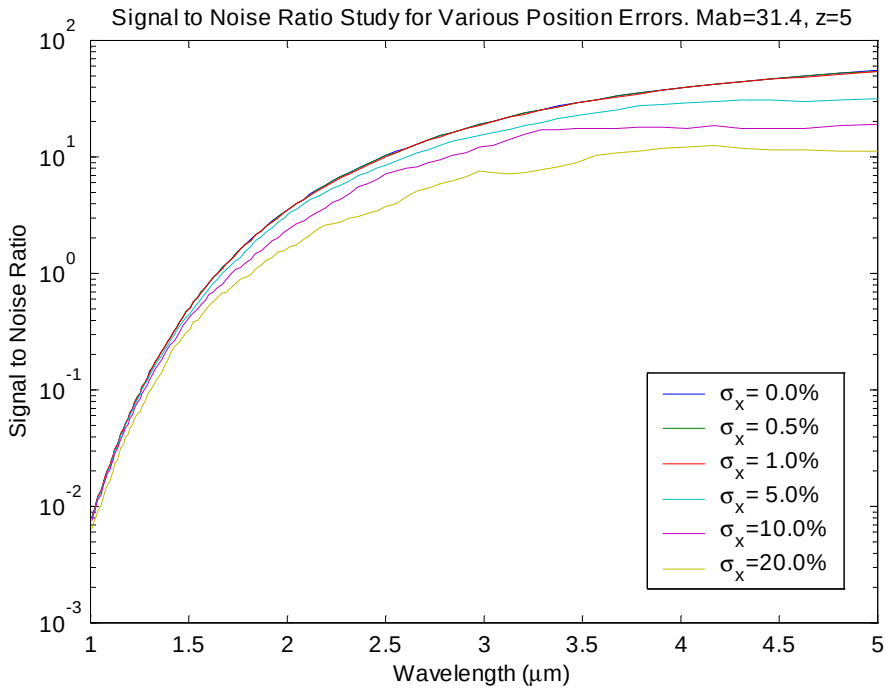

Figure 8 : Signal to noise ratio for various relative position errors (σ_x) for a faint object with an apparent magnitude of 31.4 and a redshift of 5.

3.2.5 Risk analysis and mitigation plan

While there are many approaches to assess the risk in the development of a complex instrument such as the NGST IFTS, we favour the DSMC (Defence Systems Management College) approach that was used on several NOAA programs. A team surveys the project and determines the list of all risks including both technical and management risks. The consequences of problems in terms of costs and schedules are assessed independently and the some qualitative scores are combined for each of the identified components. It therefore becomes possible to sort the risk items in priority, assign targets levels as a function of time and finally put together a risk mitigation plan. This method is described in RD 28 (Appendix B.2) and on the WWW at http:// www.dsmc.dsm.mil.

Level of Difficulty

Table 7: Level of Difficulty matrix for the various interferometer components

Component \ Environment	Thermal	Radiation	Vibration	Lifetime
Collimator	Low	Low	Low	Low
Condensor	Low	Low	Low	Low
Beamsplitter / compensator	Medium	Low	Medium	Low
Interferometer Mirrors	Low	Low	Low	Low
Sweep Mechanism	Low	Low	Medium	High
Sweep Actuator	Hard	Low	Medium	High
Metrology Source	Medium	Medium	Low	High
Metrology Fibre Optic	Medium	Medium	Medium	High
Metrology Detectors	Medium	Medium	Low	Low
Control Electronics	Low	Medium	Low	Medium

As a complement to the formal risk analysis described above, Table 7 presents a first assessment of the risks associated with IFTS broken down against the key problem factors for a space-based cryogenic instrument. The rather low risk approach of the technologies involved with the interferometer means we do not have worry about the basic feasibility.

Thermal Environment Considerations

We assume that the instrument is divided in a number of thermal zones. In Figure 7, we only show two zones, the coldest thought to be around 30 K, and another one labelled Warmer Zone. Some components will undoubtedly be located in the warmer environment. The main reason for placing a component in the warmer zone are that 1) their function allows them to be located away from the cold optics, such as electronic boards and 2) they generate heat. There is a high cost to place heat-dissipating components in the coldest environment. Current heat budgets supplied by NASA allow a few hundred mW to be dissipated by the interferometer subsystem in the 30 K area. For some components, it is not yet decided if they will be placed in the coldest zone or not. In this case they are illustrated in Figure 7 with the thermal zone border passing through them. One such example is the Sweep Actuator. From the point of view of the interferometric actuation, it would be ideal to have the actuator placed close to the sweep mechanism. However if an actuator with sufficiently low power dissipation cannot be found, a high dissipation device could be placed in the warmer area and the mechanical motion could be transferred using a stiff, insulating member, with possibly degraded actuation performance. The components for which the location is not yet known, a worst case in terms of risk is assumed, namely that they sit in the coldest zone.

Another example of component location to be determined is the Metrology Detectors. The detectors themselves will lie in the coldest zone but the associated preamplifiers may be required to be very close to the detectors to minimise noise pickup. In this case low-power design and components will be required.

The beamsplitter and compensator are made of visible and infrared light transmitting elements. Many of these materials, especially in the infrared, are relatively soft or brittle, making their mounting much harder than monolithic metal mirrors for example. This is even more of a concern in the case of cryogenic mounting and mounts appropriate for vibration (launch) environment. Both of these problems have been solved for a number of space instruments though. The level of difficulty score is thus considered medium.

The sweep mechanism would normally get a high to very high level of difficulty score, however in our baseline we assume the use of automatic alignment that alleviates the problem of distortion of the thermal structure. On the down side, this choice complicates the metrology.

The metrology fibre optic will be submitted to a high thermal gradient and this may place mechanical stresses that may not only change the light transmission characteristics but may also produce mechanical failure. However industrial fibre optics sensors are routinely used in high thermal gradient environment.

The thermal environment imposes three types of constraints on components. The first one is the difficulty of operation in a very cold environment. The second difficulty is the testing of the devices in the cryogenic chambers and the increased complexity of such operations. The third constraint is the low-dissipation requirement, almost always associated with low temperature environments.

Radiation Environment Considerations

The radiation environment has very a low level of difficulty score for all mechanical components such as mirrors (the collimator and condensor are thought to be made of mirrors and not lenses) and the sweep mechanism. The transmission properties of materials used in transmission such as the metrology fibre optic and beamsplitter/recombiner may be affected by cosmic radiation. However we consider that only the fibre optic carries a certain level of difficulty because of the long optical path and the limited choices of fibre material. As is the case for all space development, the electronic components potentially carry a significant level of difficulty associated to space radiation but we assume that we can find a solution appropriate for the level of NGST cosmic radiation. This solution will be similar to that found for the rest of the NGST system.

Vibration Considerations

A great deal of the vibration considerations in space systems are usually centred on the initial launch perturbations. This is the case for the NGST IFTS, however a Fourier Transform spectrometer requires interferometric alignment and hence also requires tolerance to vibration during operation. When an interferometer gets out of alignment, its efficiency, and consequently its sensitivity, degrades very rapidly.

The vibration environment and the thermal distortions are the factors most often cited by critics to say that the operation of a FTS in space is a risky business. This is true of FTS that *passively* rely on their structure to maintain alignment through the initial launch vibrations and through the structural deformations caused by spatial and temporal thermal gradients. The situation is different however if a FTS equipped with a *automatic or commendable* alignment system is used.

The baseline Bomem NGST IFTS has such an alignment subsystem which shares components with the metrology. The dynamic alignment utilises the light from the metrology source and adds a number of detectors alongside the metrology detectors to sense the interferometric alignment. The dynamic alignment electronics sends a signal to a pair of short-stroke actuators (such as single element piezo) to correct the alignment. This subsystem allows the system to readjust after a launch perturbation and allows compensation for thermal distortions. It allows us to design a much cheaper interferometer structure with proven space materials, to greatly reduce the “interferometer in space” risk. It also generates significant saving during testing by having this sensing device built-in the interferometer subsystem, allowing us to “see” what perturbations are experienced while the system is cooled down to 30 K. Cryogenic interferometer systems such as the CIRS on CASSINI are good examples of the challenges encountered (see Hagopian and Hagopian et al., 1996) during the cryogenic testing of a passive system.

Bomem invented the dynamic alignment more than 25 years ago.

Lifetime Considerations

Questions about lifetime in space affect 1) components with moving parts, 2) electronic components and 3) optical components in transmission. Lifetests will be performed on the sweep mechanism, sweep actuator and the alignment mechanism and actuators, all of which are moving parts.

The lifetime of electronic components in general is of concern, but the selection of space qualified electronic components is routinely performed for all space developments and does not carry

excessive risk. Special attention is to be devoted to the metrology source which is currently expected to be a solid state laser diode at 1.55 μm. We plan to select a laser diode tested for another space program at Bomem (or elsewhere) or conduct lifetests in the lab during the development.

The darkening of optical components used in transmission because of radiation is a potential problem. The material will be selected from published space-qualified lists to take care of this effect.

Risk Estimate

The risk associated with the development of an interferometer subsystem for the NGST IFTS was analysed using a standard method proposed by DSMC (Defence Systems Management College, www.dsmc.dsm.mil). This method was used to attribute a numerical risk factor to all the major components. It is important to highlight the fact that this evaluation is performed on the risk of development process failure and not on the risk of failure of the instrument in flight. An example would be, that midway in the project the optical fibre selected cannot be space qualified for cryogenic space operation. The method evaluate the risk and consequence associated with such an event and the impact of a work around solution. It is therefore assumed that the instrument will work properly once in space.

The summary of the analysis for the development of an interferometer subsystem for the NGST IFTS is given in Table 8. The three most important risk elements are found to be: 1) the sweep actuator performance, 2) the control algorithms and software and 3) the metrology source qualification. Next section addresses the mitigation of these risks.

Table 8: NGST IFTS Risk Factor

Risk No.	Item / Weighting Factors	Maturity (Pm) a 0.33	Complexity (Pc) b 0.34	Dependency (Pd) c 0.33	Probability of Occurrence (Pf) Pf = a Pm + b Pc + c Pd	Technical Factor (Ct) d 0.3	Cost Factor (Cc) e 0.15	Schedule Factor (Cs) f 0.55	Consequence (Cost of Occurrence) (Cf) Cf = d Ct + e Cc + f Cs	Total Risk (Rf) Rf = Pf + Cf - (Pf * Cf)
1	Metrology Source qualification	0.3	0.1	0.5	**0.30**	0.5	0.7	0.9	**0.75**	**0.825**
2	Cryogenic Metrology Fiber Optic Qualification	0.3	0.1	0.5	**0.30**	0.5	0.2	0.5	**0.46**	**0.617**
3	Metrology Detector qualification	0.1	0.3	0.2	**0.20**	0.5	0.3	0.5	**0.47**	**0.577**
4	Sweep actuator performance	0.8	0.5	0.5	**0.60**	0.7	0.5	0.9	**0.78**	**0.912**
5	Sweep Mechanism performance	0.5	0.5	0.3	**0.43**	0.7	0.2	0.3	**0.41**	**0.663**
6	Sweep technique performance (step scan)	0.9	0.7	0.3	**0.63**	0.5	0.3	0.5	**0.47**	**0.806**
7	Dynamic alignment performance	0.9	0.7	0.3	**0.63**	0.7	0.1	0.5	**0.50**	**0.817**
8	Dicroic system qualification	0.3	0.3	0.5	**0.37**	0.7	0.5	0.7	**0.67**	**0.791**
9	Interferometer beamsplitter qualification	0.3	0.1	0.5	**0.30**	0.7	0.4	0.3	**0.44**	**0.603**
10	Mirror qualification	0.1	0.1	0.5	**0.23**	0.5	0.3	0.3	**0.36**	**0.508**
11	input/output optics qualification	0.1	0.1	0.5	**0.23**	0.7	0.3	0.5	**0.53**	**0.639**
12	Control electronics qualification	0.3	0.5	0.5	**0.43**	0.7	0.5	0.5	**0.56**	**0.751**
13	Calibration source performance	0.9	0.8	0.3	**0.67**	0.3	0.5	0.5	**0.44**	**0.814**
14	Control software & algorithm performance	0.7	0.5	0.2	**0.47**	0.7	0.3	0.8	**0.70**	**0.837**

Mitigation Plan

Table 9 presents the result of the risk analysis and drafts a mitigation plan. A part of the mitigation plan is currently underway with the breadboard contract (pre-phase A activities). This will give The HIA/Bomem team the ability to validate some of the technology planned for the interferometer. In fact the breadboard tests will address some of the crucial aspects of risk # 4, 5, 6, 7, and 15 which include the two top risk elements. For items # 1, 3 and 10 to 13, space qualification has already been

performed on similar components on previous space instruments. These items are present in the risk evaluation because the ones required for the NGST IFTS may differ from existing space-qualified versions. It is thought that the instrument design can be modified to accommodate space qualified components.

Table 9: NGST IFTS Risk Factor and Mitigation

No.	Level	Risk Identified	Risk Mitigation planned during phase A
1	**0.825**	**Metrology Source qualification**	Assess requalification of diodes from programs with less stringent PA requirements.
2	0.617	Cryogenic Metrology Fiber Optic Qualification	Perform transmission and polarization tests at cryo temperatures
3	0.577	Metrology Detector qualification	Assess requalification of diodes from programs with less stringent PA requirements.
4	**0.912**	**Sweep actuator performance**	Perform testing on current breadboard prior to instrument design and select alternate technologies if necessary
5	0.663	Sweep Mechanism performance	Study several designs and run test on current breadboard
6	0.806	Sweep technique performance (step scan)	Perform extended testing on breadboard version
7	0.817	Dynamic alignment performance	Perform alignment by iterative optimization techniques
8	0.791	Dicroic system qualification	Research past cryogenic programs for mirror performance
9	0.603	Interferometer beamsplitter qualification	Research past cryogenic programs for mirror performance
10	0.508	Mirror qualification	Research past cryogenic programs for mirror performance
12	0.639	input/output optics qualification	Research past cryogenic programs for mirror performance
13	0.751	Control electronics qualification	Select space qualified components
14	0.814	Calibration source performance	Perform extended study and simulation of various approaches
15	**0.837**	**Control software & algorithm performance**	Test uncompiled high level version on breadboard.

3.3 Technological Readiness

Fourier transform spectrometers (FTS) are a relatively mature technology. FTS were used in space for the first time in 1962 onboard the Discoverer satellite. Since then, Fourier transform spectrometers have been used on several space platforms and FTS will be on several future missions. **Table 10** presents a partial summary of past, present and future space missions involving FTS (adapted from Persky, 1995). Use of Fourier transform spectrometers onboard aircraft, balloons, atmospheric rockets, ground vehicles and surface observatories are too numerous to list here.

Table 10 : Summary of spaceborne Fourier transform spectrometers

Name	Platform	Launch date	Mission
I6T	Discoverer	1962	Atmospheric sounding
I14, I15	Gemini 7	1965	Space, earth and celestial targets
IRIS B	NIMBUS III	1969	Atmospheric profiles
IRIS D	NIMBUS 4	1970	Atmospheric profiles
IRIS M	MARINER 9	1971	Mars survey
SI-1	Meteor	1976, 1977, 1979	Atmospheric profiles
IRIS (v)	Voyager 1 ,2	1977	Solar system survey
FS 1/4	Venera 15, 16	1983	Venus survey
ATMOS	Space Shuttle	1985, 1992, 1993, 1994	Trace gas measurements
FIRAS	COBE	1989	Cosmic background survey
CIRRIS	Space Shuttle	1991	Military mission
SPIRIT III	MSX	1996	Military mission
TES(m)	Mars Global Surveyor	1996	Mars geological survey
IMG	ADEOS	1996	Trace gas measurements
CIRS	Cassini	1997	Solar system survey
FTHSI	Migthy Sat II	2000	Military demonstration mission
MIPAS	ENVISAT	2001	Trace gas study
ACE	Sci-Sat 1	2001	Ozone measurements
IASI	METOP	2001	Atmospheric sounding
GIFT	EOS	2002	Wind velocity mapping
TES	EOS-CHEM	2003	Tropospheric trace gas study
PFS	Mars96, Mars Express	(1997) 2003	Mars survey
CrIS	NPOES	2008	Atmospheric sounding

Because of the long history of FTS in space, most of the critical factors related to space missions are well understood. For instance effects of vibrations and shocks during launch, long-term degradation of beamsplitter material due to radiation, effect of cosmic rays on FTS are relatively well understood. Several of the instruments listed in **Table 10** were cooled to cryogenic temperatures: CIRRIS (20 K), FIRAS (1.8 K), I14 and I15 (26 K), SPIRIT III (8.5 K) showing that FTS can operate at very low temperatures (Persky, 1995, Hagopian 1996).

The imaging Fourier transform spectrometer proposed in this document uses a space qualified laser diode for its metrology eliminating the problem encountered with He-Ne lasers during the first ATMOS mission. CIRS onboard the Cassini spacecraft and FIRAS onboard COBE used such laser diodes.

The design also proposes to use piezoelectric actuators to correct its alignment and a long-stroke high-resolution linear actuator, such as the Burleigh's Inchworm™ or Schaeffer Magnetics's Rubicon™ to translate its mirror. These actuators can operate in vacuum at temperatures as low as 20 K (Henderson et al., 1999) and offer the required accuracy (of the order of nanometers).

The availability of high accuracy blackbodies to be used as calibration sources in space is not a problem either. Several infrared remote sensing instruments were flown in space along with their calibration sources. For example, Bomem has built space-qualified blackbodies for the MOPITT instrument that will fly on the EOS-AM1 platform to be launched in 2000. The temperature of these

blackbodies is accurate to ±0.1 K and their emissivity is known to ±0.001 (Bouchard and Giroux, 1997).

As discussed in Sections 1, 2.3 and 3.2.4, the SNR simulations of the NGST IFTS is compatible with the current performance of the detectors arrays currently studied for NGST (McCreight, 1998). The IFTS does not require an improvement of performance in its basic operation mode, but could benefit from a detector improvement in its dispersed mode.

Manufacturing a high efficiency beamsplitter that covers the complete spectral range of NGST can be difficult depending on the width of the spectral range. However, the current proposed design can bypass this difficulty by separating the total spectral range in sub-bands using each using its own beamsplitter optimised for that band.

3.4 Breadboard Activities

The results of the trade studies have led to a design that shows two main innovations over most space and laboratory FTS. In order to study these two new aspects, namely the very slow *step scanning operation* and the *temporally separated metrology*, Bomem has proposed to build a breadboard demonstrator. The demonstrator has been designed following science requirements determined by the HIA in order to make the breadboard also usable for a meaningful ground demonstration. These requirements are described in section 3.4.1 and pertain to a large ground telescope such as Gemini or Keck. This prototype is therefore not an attempt to realize a lab version of the proposed NGST IFTS although it includes several components that are very close to what would be required for NGST.

This test bench will allow us to demonstrate our capability to successfully control these new instrument parameters and in a second phase, show the astronomical community that IFTS are well suited for space observation.

The breadboard is in the final stage of assembly and preliminary characterisation indicates that the requirements will be met (see section 3.4.3).

3.4.1 Prototype science requirements

Realizing early that the breadboard demonstrator could easily form the heart of a very attractive instrument for a ground based 8m class telescope, during a meeting held in Quebec City in March 1999, a variety of science cases were discussed in order to develop a set of science requirements for the breadboard demonstrator that would allow for this upgrade path. After much discussion, the following three science cases were settled on, focussing on visible wavelength science.

1. Dense stellar clusters - primary goal is to measure the IMF in rapidly star forming regions.
2. Nearby galaxies - primary goal is to measure abundance and star formation properties over the entire disk of some reasonably late type galaxies.
3. Rich clusters of galaxies - primary goal is to do photometric redshifts and possible also Lyman alpha searches at high redshift, but will also use a moderate redshift cluster to (a) act

as a lens, and (b) give us lots of cluster science (e.g. galaxy star formation as a function of radius, cluster substructure, etc).

These science cases were then translated into the science requirements listed in.

Table 11 : Breadboard Requirements

Item	Goal	Required
Wavelength range	0.32 – 1.0 µm	0.35 – 0.9 µm
Telescope	8m primary, f/16, instrument located at Cassegrain (changing gravity vector)	Idem
FOV	6.8 arcmin	Idem
Pixel FOV	0.1 arcsec (i.e. 4k detector)	0.2 arcsec (i.e. 2k detector)
Spectral Resolution	Up to R=5000	Up to R=1000
Throughput	0.5 @ 0.5 µm (including CCD)	Idem
Port design	4 port (2 output camera)	Idem
Filter wheel	5 filters remotely changeable	none

The breadboard design described in section 3.4.2 satisfies these requirements.

3.4.2 Prototype design and hardware

Metrology system

As demonstrated from the performance simulation, the accuracy of the interferogram sample positions is a requirement affecting the sensitivity of the instrument. It has been shown that OPD errors of 1 % on the sampling interval, are required to produce optimum SNR. This concern is of even greater interest for NGST since the OPD stability has to be maintained for long periods of time. The OPD stability requirement is given in terms of percentage of error on the sampling position. According to the Nyquist/Shanon theorem, in order to measure spectrum down to the UV (300 nm) the interferogram has to be sampled at twice the highest frequency; i.e. at 150 nm. This means that the sweeping mirror has to be moved by OPD increments of 150 nm. In a standard interferometer design, the optical path length in one arm is twice the distance between the mirror and beamsplitter since the light goes back and forth along the way. A given displacement on the sweeping mirror produces twice as much optical displacement. The steps of 150 nm OPD in this case correspond to mechanical steps of 75 nm of the moving mirror. Our requirement of 1% on the sampling interval translates for the prototype into acceptable errors equivalent to 0.75 nm on the position of the mirror during integration of the science light. It is important to underline that this prototype requirement is more than three times more stringent than for the actual NGST core spectral range 1 – 5 µm :$\left(\frac{1\% \cdot 1\mu m}{2 \cdot 2} = 2.5nm\right)$.

The challenge is to measure the OPD with such precision. Some commercial position sensor can monitor absolute position with similar precision but their range is limited to microns. Other sensors with greater range, such as the Burleigh Inchworm™ are available with an integrated

encoder, but cannot achieve the required absolute sub nanometer accuracy. Moreover, it is important to mention that only looking at the displacement of the moving mirror cannot monitor the true OPD. Thermal gradients between both paths in the interferometer as well as beamsplitter or fixed mirror also influences OPD. Even though these two elements intent to be tightly secured to the structure, at sub nanometer resolution, vibration effects cannot be ignored and OPD has to be monitored by looking at both optical path in the interferometer. This has led to the design of a laser metrology system that provides both unrestricted range and absolute sub-nanometer monitoring of the true OPD. The most direct method is used, i.e. by injecting a laser signal in the interferometer along the science light, both beams suffering exactly the same OPD variations. In the prototype, the metrology is injected in the centre of the interferometer pupil to allow the reuse of proven metrology designs. In the flight design, the metrology would probably be off centre to avoid obscuration. The breadboard metrology system monitors OPD with an absolute accuracy of 1 nm optical or 0.5 nm mechanical.

This metrology system is proposed for the flight instrument to accurately find the sampling positions. The metrology detectors provide feed back to drive a fine OPD actuator. This allows very precise and rapid positioning (less than 1 second including stabilisation time).

For NGST, we propose to shut off the metrology while the science integration takes place. On the breadboard we will test the OPD stability with disengaged metrology i.e. by turning the servo feedback off while leaving the metrology on. This will enable us to characterise the system stability and compare it with our simulations and FEM analyses.

It is expected that the ground-based environment will cause more OPD instabilities than in space. The presence of air in both arms of an interferometer affect the OPD (Grandmont & Moreau, 1998) in a way negligible for fast sweeping systems but critical for step scanned interferometers such as the one for NGST with individual integration times of the order of minutes. In order to approach NGST conditions, the system will be studied for OPD stability in an air-controlled environment.

To make the breadboard even more robust when mounted on a ground telescope, the metrology was designed with a laser diode at 1.55 µm for it to operate in a spectral region separated from the response of the CCD science detectors. It will then be possible to maintain the OPD servo on while acquiring optical science data. This option is obviously not being considered for NGST observations in the 1 to 5 µm range.

Another task of this innovative metrology system is to sense the interferometric alignment in order to provide feed back to a pair of alignment actuators and ensure the highest modulation possible over the full FOV. Automatic interferometric alignment was introduced in the original Bomem interferometers more than 25 years ago. For the NGST instrument, the same method is proposed with modifications in the way the wavefront is sensed in order to adapt it for step scan operation mode. In the current version, the metrology system is able to tell the OPD and alignment, and hence correct for both at a rate of 1 kHz. This rate is directly related to the speed at which the system can reposition itself properly between integrations.

Sweep mechanism

When air is removed from inside the interferometer, the sources of OPD errors left are the relative motion of the fixed mirror, scanning mirror and beamsplitter. Thermal distortions of the structure holding these components can also change the OPD. These perturbations depend on the thermal environment (relatively benign in NGST, more difficult in the uncontrolled environment of a ground telescope) and are slow, on the order of the thermal response of the system. The other sources of distortion are the vibrations. Here the instrument must be designed to be very stiff so it can passively reject these perturbations. In the breadboard the effect of the vibrations in the transverse directions are mitigated by the finite element modelling that has been performed on the sweep mechanism of the CrIS mechanism which is nearly identical to that of the breadboard besides the actuators. Bomem is currently developing the CrIS interferometer module for ITT, the prime contractor of the CrIS Program (http://192.64.69.136/S_cris.htm).

The fixed mirror and beamsplitter are firmly secured into the interferometer structure, which is a rigid monolithic bloc of aluminium machined of hexagonal shape (see Figure 9). This structure is derived from early Bomem field interferometer. The item that is undoubtedly the most sensitive to vibrations is the sweep mechanism holding the moving mirror. It is designed with the highest stiffness possible in the direction of motion. In fact, the actuator is the only item restricting the motion in the sweep direction. The commercial actuator chosen for the breadboard, the Burleigh Inchworm™, provides the stiffness required (~5 N/µm) to push the sweep resonance frequency above 100 Hz (design goal).

The current baseline uses a space qualifiable Bomem/ITT sweep mechanism. The mechanism is balanced so as to be immune from linear vibration including the direction of motion of the moving mirror. It also has the benefit that the instrument can operate on earth in any orientation without changing the force applied on the sweep actuator head.

The NGST IFTS design also benefits from life tests currently underway for two versions of the CrIS sweep mechanism, having already demonstrated its performance over 15 millions of sweep cycles. At its slow scan rate, the NGST instrument is expected to perform many times fewer cycles than this value. It will be necessary to repeat these tests at cryogenic temperature for the NGST mechanism, but the room temperature results provide invaluable data towards space qualification.

Resistance to shock and vibrations is another important factor. Here again there exists a wealth of data from past airborne FTS campaigns. Many studies are being performed on cryogenic versions of piezos. This is one of the reasons why the Inchworm was chosen as the main OPD actuator in the breadboard design..

Optical design

An IFTS can support the geometrical throughput of an 8-meter class telescope. The interferometer pupil required for NGST is approximately 12 cm. For the breadboard, in order to save cost and shorten development time, we elected to use a standard Bomem beamsplitter format providing 8 cm of interferometer pupil. The rest of the components including the sweep mechanism, metrology source and detectors can be use as is for an 8m telescope and 5.2 by 5.2 arcmin FOV. The 8 cm beamsplitter is matched to a 6m 4.5 x 4.5 arcmin FOV telescopes, quite

an achievement for a short schedule and low cost breadboard. This level of realism should make the demonstration of the feasibility of the NGST IFTS much more convincing. The breadboard will also support quite easily upgrades to a full NGST étendue by retrofitting a new beamsplitter and support structure. The other components can be reused without modification.

Hardware

Figure 9 shows an exploded view of the interferometer with all its components. In addition to this set-up, a user interface console and the actuator drivers, which are not shown on this picture, are required to run the interferometer. The complete interferometer fits in a box with the following dimension: 50 cm X 40 cm X 35 cm. This does not include input/output optics, science detectors or their electronics.

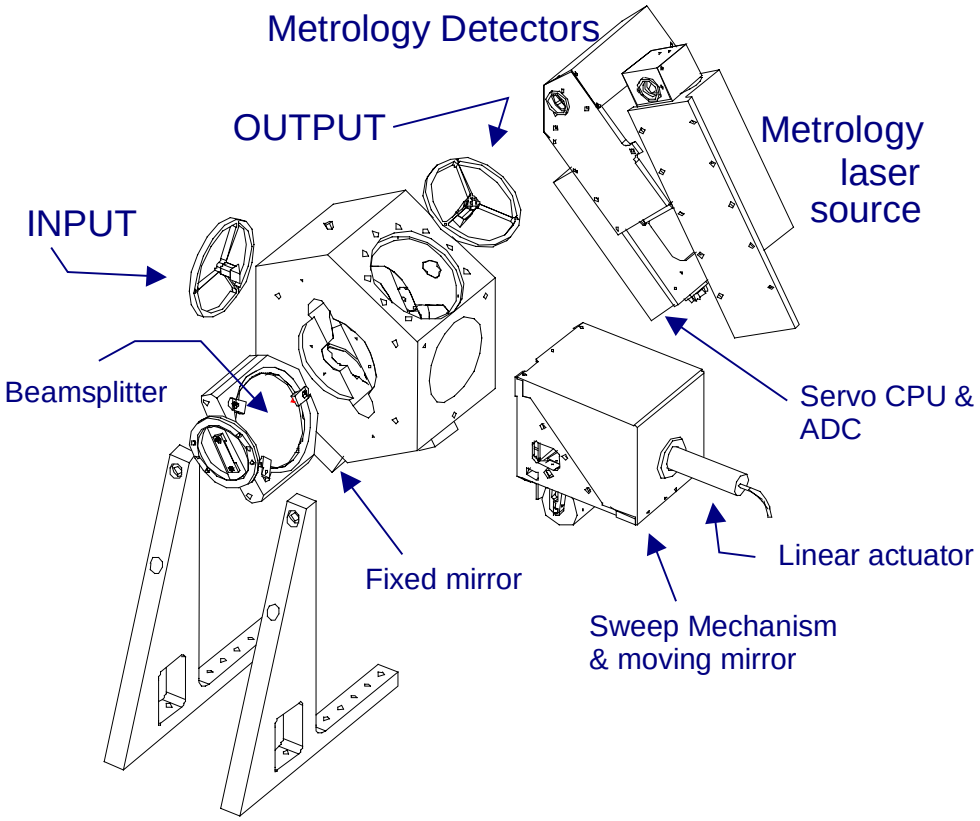

Figure 9 : Exploded view of the prototype

Figure 10 shows how all the spectrometer components interact with each other. In this prototype, the metrology is inserted in the middle of the science light with folding mirrors held by spiders visible at the input and output on Figure 9. The obscuration caused by these folding mirrors and their support is less than 5 %.

Dynamic alignment is performed directly on the sweeping mirror by piezo actuators similar to the one used for OPD correction. In the breadboard, the Inchworm is used to provide coarse positioning.

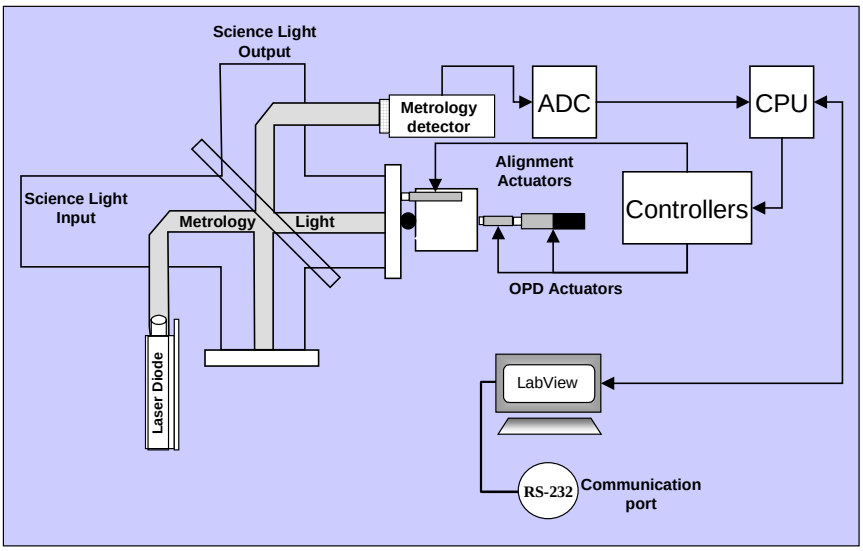

Figure 10 : Block diagram of the breadboard

3.4.3 Prototype test plan and results

As of 1 October 1999, the prototype is entering the characterisation phase. Figure 11 shows the final assembly of the system. The integration into an operational instrument that can be fitted to a ground telescope is expected to begin in late October. For this demonstration phase, Bomem is teaming with LLNL. This integration includes the production by LLNL of input and output optics that will bring the telescope light to fit into the 8 cm aperture IFTS. LLNL will also provide the science detector array and electronics. Results from astronomical observations are expected in late December 99.

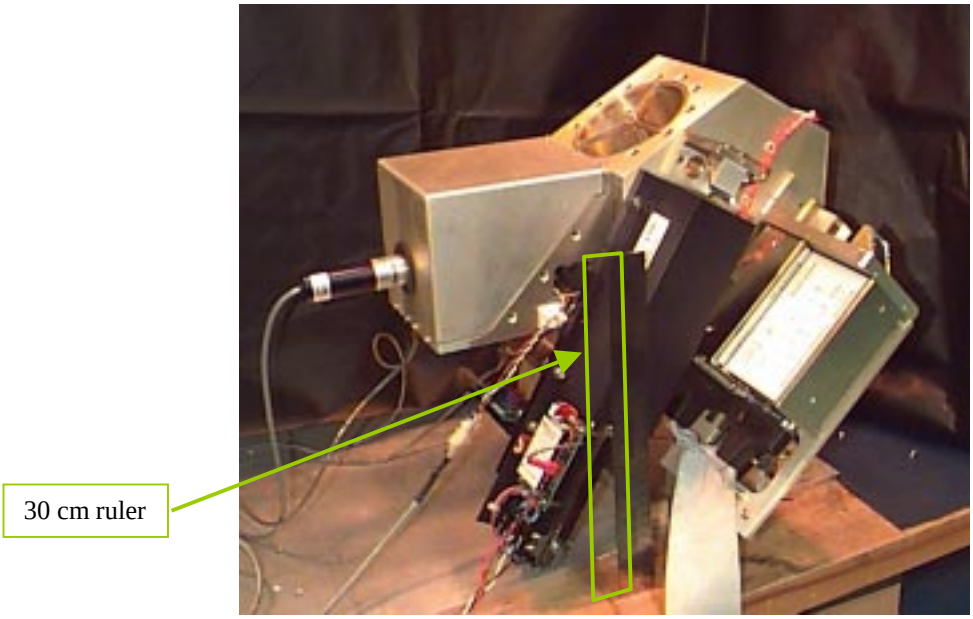

Figure 11 : Prototype picture

The stiffness of the sweep mechanism has been experimentally evaluated at 1.8 N/µm. This value is consistent with the prediction and is sufficient to meet the requirement of ground based telescopes. The stiffness would be higher for NGST since the breadboard includes an additional piezo actuator (not needed for NGST) that simplifies the OPD servo design but also reduce the stiffness somewhat. It is not impossible either that a stiffer version of the Inchworm or an altogether different actuator could be used for NGST.

The first stability data obtained show that the system is passively stable within 10 nm optically over period of time of 5 minutes in an uncontrolled environment (exposed to air drift and lab vibrations). The addition of a temperature control system will bring this value down to the required 1.5 nanometer. The sweep mechanism shows a resonance at a frequency of 110 Hz.

The overall weight of the system including all electronics (except for piezo driver and control computer) is approximately 50 lbs. No effort has been made however in the breadboard to reduce mass. The hexagonal structure, which accounts for a great portion of the mass, could be weight relieved greatly.

3.5 Development schedule and integration test plan

The contribution from Canada to a NGST IFTS was assumed to be as a subcontractor to a prime instrument contractor. The scenario involves having Bomem deliver a space qualified interferometer module for integration in the instrument. The development schedule thus reflects this assumption and introduces schedule milestones slightly different than for a complete instrument provider.

Various approaches are possible for the development of space hardware as far as models are concerned. The model philosophy typically flows down from the risk analysis which can be done in a quantitative way, with targets set for the various models and to achieve an acceptable risk for the flight unit. Obviously, the mission criticality of the sensor, the overall mission (launch and platform) costs also fold in. We expect that the NGST expectations will be very high, typical of the larger science missions like EOS or ENVISAT. A high probability of success is required. This assessment implies that:

- Strict PA requirements will be enforced
- Rigorous development methods must be followed
- Reviews, control boards etc. will be implemented
- Risk reduction programs will be developed
- Mass models will be supplied
- Simulators will be used for verification throughout

We propose a development approach that uses basically three key models, 1) a breadboard which is currently under development, 2) an engineering model which will be form, fit and function compatible with the flight model but may use lower grade of space qualification on the electronics, and 3) a flight model.

To maintain reduced cost and accelerated development, the development approach will reuse available components as much as possible and make use of synergies with other space programs. Figure 12 shows the proposed NGST IFTS schedule (bottom - ID 20 and higher) along with the NGST milestones (top – ID 1-19). The schedule was constructed around four milestones provided by CSA, the NGST IFTS Kickoff, FM PDR, FM CDR and delivery.

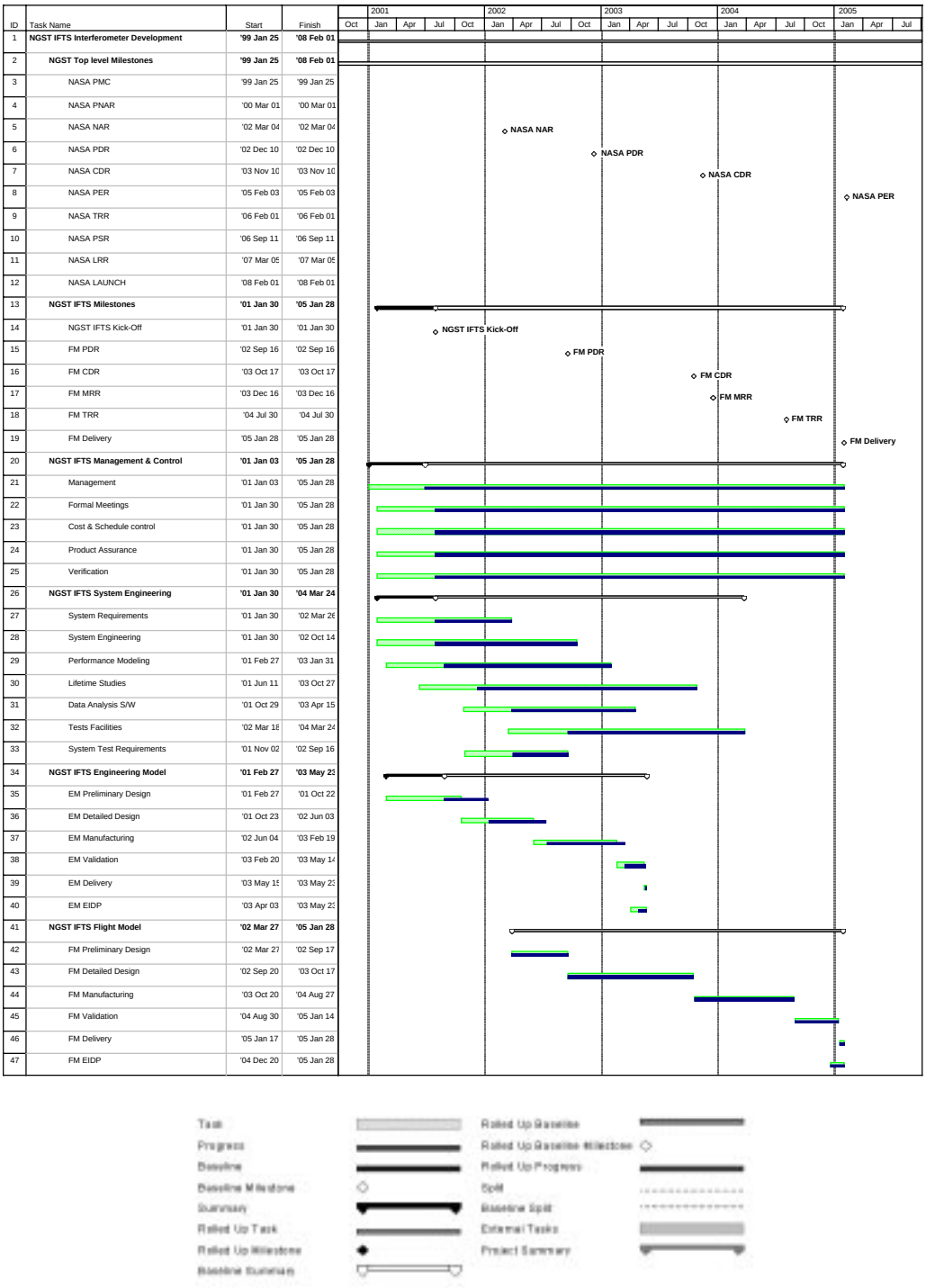

ID	Task Name	Start	Finish
1	**NGST IFTS Interferometer Development**	**'99 Jan 25**	**'08 Feb 01**
2	**NGST Top level Milestones**	**'99 Jan 25**	**'08 Feb 01**
3	NASA PMC	'99 Jan 25	'99 Jan 25
4	NASA PNAR	'00 Mar 01	'00 Mar 01
5	NASA NAR	'02 Mar 04	'02 Mar 04
6	NASA PDR	'02 Dec 10	'02 Dec 10
7	NASA CDR	'03 Nov 10	'03 Nov 10
8	NASA PER	'05 Feb 03	'05 Feb 03
9	NASA TRR	'06 Feb 01	'06 Feb 01
10	NASA PSR	'06 Sep 11	'06 Sep 11
11	NASA LRR	'07 Mar 05	'07 Mar 05
12	NASA LAUNCH	'08 Feb 01	'08 Feb 01
13	**NGST IFTS Milestones**	**'01 Jan 30**	**'05 Jan 28**
14	NGST IFTS Kick-Off	'01 Jan 30	'01 Jan 30
15	FM PDR	'02 Sep 16	'02 Sep 16
16	FM CDR	'03 Oct 17	'03 Oct 17
17	FM MRR	'03 Dec 16	'03 Dec 16
18	FM TRR	'04 Jul 30	'04 Jul 30
19	FM Delivery	'05 Jan 28	'05 Jan 28
20	**NGST IFTS Management & Control**	**'01 Jan 03**	**'05 Jan 28**
21	Management	'01 Jan 03	'05 Jan 28
22	Formal Meetings	'01 Jan 30	'05 Jan 28
23	Cost & Schedule control	'01 Jan 30	'05 Jan 28
24	Product Assurance	'01 Jan 30	'05 Jan 28
25	Verification	'01 Jan 30	'05 Jan 28
26	**NGST IFTS System Engineering**	**'01 Jan 30**	**'04 Mar 24**
27	System Requirements	'01 Jan 30	'02 Mar 26
28	System Engineering	'01 Jan 30	'02 Oct 14
29	Performance Modeling	'01 Feb 27	'03 Jan 31
30	Lifetime Studies	'01 Jun 11	'03 Oct 27
31	Data Analysis S/W	'01 Oct 29	'03 Apr 15
32	Tests Facilities	'02 Mar 18	'04 Mar 24
33	System Test Requirements	'01 Nov 02	'02 Sep 16
34	**NGST IFTS Engineering Model**	**'01 Feb 27**	**'03 May 23**
35	EM Preliminary Design	'01 Feb 27	'01 Oct 22
36	EM Detailed Design	'01 Oct 23	'02 Jun 03
37	EM Manufacturing	'02 Jun 04	'03 Feb 19
38	EM Validation	'03 Feb 20	'03 May 14
39	EM Delivery	'03 May 15	'03 May 23
40	EM EIDP	'03 Apr 03	'03 May 23
41	**NGST IFTS Flight Model**	**'02 Mar 27**	**'05 Jan 28**
42	FM Preliminary Design	'02 Mar 27	'02 Sep 17
43	FM Detailed Design	'02 Sep 20	'03 Oct 17
44	FM Manufacturing	'03 Oct 20	'04 Aug 27
45	FM Validation	'04 Aug 30	'05 Jan 14
46	FM Delivery	'05 Jan 17	'05 Jan 28
47	FM EIDP	'04 Dec 20	'05 Jan 28

Figure 12: GST IFTS Schedule

The resulting schedule is quite aggressive and is thought to increase the risk of the development. There is only a four-month period between the kickoff and PDR of the EM. This is especially short considering that during that time a large development team (>25) has to be built. The work performed on the breadboard (pre-phase A) will help quickly come to a technological baseline for the EM, but the proposed schedule is thought to be restrictive, We would recommend to increase the timeframe by 20-40% if it is possible, by example starting the EM program earlier, perhaps at a reduced effort. Both schedules are displayed in Figure 12.

4. Cost estimate

REMOVED ACCORDING TO A DIRECTIVE FROM THE CANADIAN SPACE AGENCY

5. References

RD 1 Abraham R. G., "Quantitative Morphology at High Redshifts", astro-ph/9802036, 1998.

RD 2 Alcock C., R. A. Allsman, D. Alves, T. S. Axelrod, A. C. Becker, D. P. Bennett, K. H. Cook, K. C. Freeman, K. Griest, J. Guern, M. J. Lehner, S. L. Marshall, B. A. Peterson, M. R. Pratt, P. J. Quinn, A. W. Rodgers, C. W. Stubbs, W. Sutherland, & D. L. Welch., "The MACHO Project Large Magellanic Cloud Microlensing Results from the First Two Years and the Nature of the Galactic Dark Halo ", ApJ, 486, 1997.

RD 3 Bouchard R. and J. Giroux, "Test and qualification results on the MOPITT flight calibration sources", Opt. Eng., 36 (11), 1997.

RD 4 Burrows A., M. Marley, W. B. Hubbard, J. I. Lunine, T. Guillot, D. Saumon, R. Freedman, D. Sudarsky, & C. Sharp, " A Nongray Theory of Extrasolar Giant Planets and Brown Dwarfs ", ApJ, 491, 1997.

RD 5 Carlberg, R. G., H. K. C. Yee, S. L. Morris, H. Lin, E. Ellingson, D. Patton, M. Sawicki, C. W. Shepherd, "The Omega_M-Omega_Lambda Dependence of the Apparent Cluster Omega", ApJ, 516 (2), 1999.

RD 6 Genest J. and P. Tremblay, "NGST Final Report – Volume 5 : Technology Report", SP-BOM-07/99 , Bomem and Laval University, 1999.

RD 7 Graff D. S. and K. Freese, "Analysis of a Hubble Space Telescope Search for Red Dwarfs: Limits on Baryonic Matter in the Galactic Halo", ApJL, 456 (49), 1996a.

RD 8 Graff D. S. and K. Freese, "The Mass Function of Low-Mass Halo Stars: Limits on Baryonic Halo Dark Matter ", ApJL, 467 (65), 1996b.

RD 9 Graham J. R., M. Abrams M., C. Benett, J. Carr, K. Cook, A. Dey, R. J. Hertel, N. H. McCoy, S. L. Morris, J. Najita, A. Villemaire, E. Whishnow and R. Wurtz, "An Integral Infrared Spectrometer for the Next Generation Telescope", NGST instrument team report, 1999.

RD 10 Graham J. R., M. Abrams M., C. Benett, J. Carr, K. Cook, A. Dey, J. Najita, and E. Whishnow "The Performance and Scientific Rationale for an Infrared Fourier Transform Spectrograph on a Large Telescope", Pub. Of the Astro. Soc. of the Pacific, 110, 1998.

RD 11 Grandmont F. and L. Moreau "Spectral Imager (SPIM): Experimental Report", SP-BOM-20/98 , Report to the Canadian Space Agency, Bomem, 1998.

RD 12 Hagopian J. G., "Cryogenic optical alignment stability (COAST) of the Composite Infrared Spectrometeter (CIRS) for the Cassini mission to Saturn", SPIE 2814, 1996.

RD 13 Hagopian J. G. P. A. Hayes, J. A. Crooke, J. J. Lyons III, A. Morell, T. French, M. Hersh, C. Lashley, and S. S. Schmidt, "High-stability adjustable cryogenic-compatible beamsplitter

mounts for the Composite Infrared Spectrometer (CIRS) for the Cassini mission to Saturn ", SPIE 2814, 1996.

RD 14 Hansen B. M. S., "Cooling Models for Old White Dwarfs ", ApJ, 520, 1999.

RD 15 Hashimoto,Y.,A. Oemler, H. Lin, and D. L. Tucker, "The Influence of Environment on Star Formation Rates of Galaxies", ApJ, 499, 1999.

RD 16 Henderson D. A., J. C. Fasick and F. Duver, "INCHWORM Motor Design For The NGST", NGST Science and Technology Exposition, Hyannis, 1999.

RD 17 Ibata R. A., H. B. Richer, R. L. Gilliland, D. Scott, " Faint, moving objects in the Hubble Deep Field: components of the dark halo?", accepted for publication in ApJ Letters

RD 18 Kauffman G., "Clustering of Galaxies in a Hierarchical Universe: II. Evolution to High Redshift", astro-ph/98-9168, 1998.

RD 19 McCreight C., "Detector Technology Development for NGST", NASA Ames presentation, 1998.

RD 20 Moreau L. and F. Grandmont, "NGST Final Report – Volume 3 : Trade Analysis", SP-BOM-07/99 , Bomem, 1999.

RD 21 Moreau L. and P. Tremblay, "NGST Final Report – Volume 4 : Performance Analysis", SP-BOM-08/99, Bomem and Laval University, 1999.

RD 22 Pascarelle S. M., R.A. Windhorst, W.C. Keel, and S.C. Odewah, "Sub-galactic clumps at a redshift of 2.39 and implications for galaxy formation" , Nature, 383 (6595). 1996.

RD 23 Persky, J. M., "A review of spaceborne infrared Fourier transform spectrometers for remote sensing", Rev. Sci. Instrum., 66 (10), 1995.

RD 24 Revercomb H. E., AERI project, U. of Wisconsin, private communication, 1999.

RD 25 Revercomb H. E., H. Buijs, H. B. Howell, D. D. Laporte, W. L. Smith, and L. A. Sromovsky, "Radiometric calibration of IR Fourier transform spectrometers: solution to a problem with the High-Resolution Interferometer Sounder", Appl. Opt., Vol. 27, No 15, pp. 3210–3218, 1988.

RD 26 Saumon D. and S. B. Jacobson "Pure Hydrogen Model Atmospheres for Very Cool White Dwarfs ", ApJL., 511 (107), 1999.

RD 27 Stockman H. S., D. Fixsen, R. J. Mather, M. Nieto-Santisteban, J. D. Offenberg, R. Sengupta, S. Stallcup, "Cosmic ray rejection and image processing aboard the Next Generation Space Telescope ", Proceeding of the 34th Liège Astrophysics Colloquium: NGST: science drivers and technological challenges, (ESA SP-429), June 1998.

RD 28 Villemaire A, J. Bergeron and F. Grandmont, "NGST Final Report – Volume 2 : Planning Report", SP-BOM-06/99, Bomem, 1999.

Appendix A.1 Answers to the Pre-Woods Holes questions to instrument study teams

Q1. ***What are the possibilities for hybrid instruments with dispersive devices, tuned filters, and slits?***

A1. A dispersive element such as a prism can be inserted in the optical path of an imaging Fourier transform spectrometer. Graham et al., has described such an hybrid instrument in their final report. In most case the operation of a dispersed FT will also require a slit mask at the entrance focal plane. Such an hybrid IFTS will have an improved sensitivity at fine spectral resolution at the price of increased complexity, risk and cost. Alternatively a filter wheel can be introduced in the optical path. Narrow bands filters are used to reduce the photon noise and study fainter targets in a reduced spectral band.

Q2. ***Is there an important difficulty with data rate, or is there a simple form of on board data compression (or data rejection) that reduces this greatly?***

A2. In the event that the data rate required to transfer the full datacube (one interferogram for every pixel of the field of view) is too high, that data rate can be reduced by several means. First the data rate can also be reduced by the use of lossless data compression methods adapted to interferograms (decimation, bit trimming, differential encoding, etc.). The compression factor depends strongly on the spectral bands and spectral features of the objects; compression factors between 2 and 50 are typical. Alternatively, onboard computers can process the interferograms into spectra which allows only the points of interest to be transmitted. This has been done in the past, for instance with the FS 1/4 onboard Venera 15 and 16 and is now common practice for ground and airborne instruments. Finally, spatial sub-sampling (dropping the data from pixels deemed to carry information of less importance) and reduced spectral resolution are further ways to reduce the data rate. It is important to note that if we agree on the final data products, the data rate from any instrument should be similar.

Q3. ***What choice of image scale are available, and why? Can these be changed in flight?***

A3. The Bomem/HIA study concentrated on the interferometer subsystem, and the feasibility of selectable focal length and corresponding plate scales has not been studied. On the other hand the interferometer is only composed of plane parallel optics and can accommodate plate scales just as easily as the filter wheel assembly on a imager. The only additional design guideline for the IFTS is to respect the obliquity criterion, i.e. to make sure that the single pixel maximum divergence is respected. This is described in Section 3 of Appendix B.4.

Q4. ***What broad or narrow band filters would be provided, where and why?***

A4. The use of narrow band filters is very common in both ground and space IFTS designs. These filters are useful to reduce the photon noise and study fainter targets in a reduced spectral band. They can also be used to acquire broadband images in spectral range familiar to astronomers when the IFTS is used as a camera. The addition of such a filter wheel has a minimal impact on the interferometer subsystem design.

Q5. ***What are the consequences of cosmic ray hits?***

A5. Due to its broadband nature, IFTS tend to be less susceptible to cosmic ray hits because of the larger science signals usually present on each pixel. The effect of an *uncorrected* cosmic ray hit does however manifest itself rather differently in a IFTS spectrum than in a spectrum from a dispersive

instrument. Some have argued that this is beneficial for the IFTS some have argued the reverse. Detailed simulation would be required to conclude on this topics. However the baseline is to correct for these cosmic events. Cosmic ray hits can be rejected by using the multiple non-destructive read method described by Stockman et al., 1998 for NGST wide field imaging. The complementary detector sets of a four-port interferometer also offers interesting possibilities to correct corrupted data points.

Q6. How can higher spectral resolution be achieved?
A6. The ultimate spectral resolution and also the flexibility to choose freely the spectral resolution within the available range is one of the strength of the FTS design. The resolution depend on the maximum optical path difference achieved between the two mirrors of the interferometer. The longer the path is, the finer the spectral bins are. The design criterion to analyse when designing the IFTS is the divergence of the light associated with each pixel. We have found that our NGST IFTS design intrinsically supports R=20,000 with no difficulties at all. The maximum *usable* spectral resolution depends on the desired signal to noise ratio and on the radiometric flux of the target. As mentioned in A1, the use of a standard dispersive spectrometer coupled to an IFTS can also increases the sensitivity of high spectral resolution measurements.

Q7. ***How many objects of each type can be seen in a reasonable time, and why is it interesting to see this many? How many different types can be studied?***
A7. An IFTS can survey the complete field of view of NGST and capture all the objects in this field. An IFTS does not take more time to survey the complete field of view than to survey a sub-sample of that field. The time of observation is set by the level of flux of the faintest object of interests and the desired signal to noise ratio. It is interesting to be able to survey the complete field of view, because one of the goals of NGST is to discover new phenomena that no one can predict today. The number of object will vary with the specific science goal, see Section 2 for several examples.

Q8. ***As the FTS is also a camera, is there a way to use one or more parts of the detector to provide guidance information to the Fast Steering Mirror while the instrument is running?***
A8. In principle it is possible to use the IFTS science detectors to guide the Fast Steering Mirror. However this approach imposes a new set of requirements (bandwidth, windowing, etc.) on the science requirements that may be better served in a dedicated sensor. Furthermore the use of the science detectors for fast steering guidance may require the use of both sets of detectors in the four-port interferometer scheme, to combine the measurements and separate the interferometric modulation from the guidance information, although this does not seem to be necessary in the first analysis.

Q9. ***Is a coronographic option available?***
A9. The coronographic option has not been studied in our work. Being quite decoupled form the interferometer operation, this option is thought to be supportable with no impact on the current design.

Q10. ***How will the instrument be calibrated in the development phase? After integration on the ground? In flight? What standard objects can and must be seen? Is calibration an automated part of the operation?***
A10. As already mentioned FTS have a clear calibration advantage over dispersive spectrometers (see Appendix A.2). During the development and integration phase, absolute radiometric calibration and spectral characterisation is performed with high accuracy blackbodies and spectral references such as gas cells. The current design includes, as part of the flight operational scheme, a regular

calibration process using a onboard blackbody sources. Observation of standard objects is not necessary for calibration but can be useful for *verification* of the onboard calibration system and evaluate the changes in the spectral reflectance of the primary mirror of the telescope.

Q11. ***How good must the detectors be? Efficiency, read noise, dark current, cosmetic defects, electronic stability, self glow?***
A 11. All of the sensitivity simulations for non-dispersed IFTS, from us and the IFIRS team, assume current-day detector performance and unlike dispersed spectrometers demonstrate the tolerance of the IFTS to detector imperfections.

Q12. What stability is required?
A12. Referring to *mechanical* stability, the current IFTS design has been developed so as to meet the performance requirements in an environment that suffers the vibration level typical of *ground* telescopes. It is expected that the vibration level of NGST will be lower. The stiffness of the breadboard could also easily be improved since it is driven by the actuators and a commercial item with no customisation was used. Bomem has designed and operated IFTS on propellers and jet aircraft that have more intense vibrations than NGST will have.

Q13. ***How many essentially different mode of operations are there? (i.e. how many different experts and sets of software are required to run and calibrate the instrument)*.**
A13. The interferometer subsystem has only one mode of operation, even if the spectral resolution can be adjusted continuously from R=1 to R>10,000. The operation involves commuting the metrology source on, servo controlling the OPD actuator to the next sampling position. Perform interferometric alignment using the same metrology signals. Clamp the actuators to their stabilised values and commute the metrology source off. The operation of the interferometer is interrupted until the integration on the science detectors is finished and the next OPD is commanded. The control software needed for the interferometer can be implemented in a CPU with a modest processing power, in a similar way as described in Section 3.4.3. The selection of the radiometric calibration using onboard sources would be controlled by a separate system-level control software.

Q14. ***What dithering patterns are required to cross calibrate the detector gains and flat field? To fill in gaps? Note that dithering is natural to for cameras and IFTS, not for some kinds of spectrographs.***
A14. The individual gains and offsets for the each detector element is determined by a calibration method that uses measurements of the onboard calibration sources and don't require dithering. See Appendix A.2.

Q15. ***What requirements and advantages and risks are there for remote adjustment devices like focussing and alignment?***
A15. The Bomem/HIA study concentrated on the interferometer subsystem, and not on focussing optics. Since the interferometer is composed on plane parallel optics only, focussing of fore or aft optics has no impact on the interferometer module. It is planned to have internal alignment to preserve the optimum performance of the interferometer, but this alignment capability is not available to steer to field of regard or correct for perturbations external to the interferometer.

Q16. ***Are there single point failure risks?***
A16. The IFTS has one macroscopic moving component (moving mirror) and two additional small tilt correction actuators. The IFTS moving mirror is a single point failure risk, but such a failure would allow to continue using the IFTS as a camera with no degradation in panchromatic

performance. The proposed sweep mechanism uses flexure blades and a good immunity to failures can be obtained by designing redundancy in the actuators. The IFTS can operate, although without any direct accuracy feedback, if the internal metrology fails. It would be fairly easy to use a bright source and the science detectors to maximise the interferometric alignment. A similar approach could be used to characterise the OPD steps. In the event that multiples detectors are used to cover a wider spectral range, every IFTS serving a given band would be independent of the others. Considering that the current design can be a dual output port system, the instrument would operate with an efficiency reduced by factor $\sqrt{2}$ if the detector of one output port fails.

Q17. ***Do the required detectors wear down with time, due to age, chemical attack on the ground or cosmic rays?***
A17. Our team did not study this question.

Q18. ***How might the choice of ISIM construction materials affect the design, operations, and stability of the instrument?***
A18. Ultimately, the proposed instrument requires an stable environment (stable to a few tenths of degrees Kelvin) with a temperature lower than 40-70 K. The vibration level should not be higher that the vibration level typical of ground telescopes. Due to the proposed auto-alignment mode, the general requirements imposed by the IFTS are greatly relaxed.

Q19. ***Assuming that mass is a limiting factor in the overall ISIM, how can the design be altered or descoped to minimize mass with less harm to the science potential?***
A19. Our findings indicate that we can build a IFTS using a volume and space constraints similar to those of a filter wheel but with much greater science return. Most descoping that can be achieved however are at the system level, mainly detector and optics options. Changing the two output ports design to a single output port design would remove one detector per band and remove some optical elements, reducing the mass and the cost but also reducing the efficiency by a factor $\sqrt{2}$. Limiting the spectral range of NGST to a range that can be covered by a single detector array will eliminate the IFTS elements used to cover the various bands, reducing the total mass and cost dramatically. If it is acceptable to have a lower efficiency outside the 1 μm to 5 μm range, the design can also be reduced to single IFTS to cover to whole spectral range of all the detectors. In that last case, the reduced efficiency near the limits of the spectral range will be due to the difficulty of manufacturing a beamsplitter to cover a wider spectral range. The efficiency in the 1 μm to 5 μm band would not be affected.

Q20. ***More generally, given that cost will be an overall limiting factor in the overall ISIM, how can the design be altered or descoped to minimize cost with least harm to science potential?***
A.20 The answer to question 19 also apply to cost.

Appendix A.2: Calibration of a FTS

One of the strengths of FTS is the ease with which one can calibrate their output into physical calibrated units. Because of the way the interferogram sampling is usually achieved, i.e. with a laser etalon, FT spectra usually show the most accurate and most stable spectral scale (X-axis). The irradiance or radiance scale (Y-axis) can also be calibrated with very low levels of systematic errors as demonstrated in Figure 13.

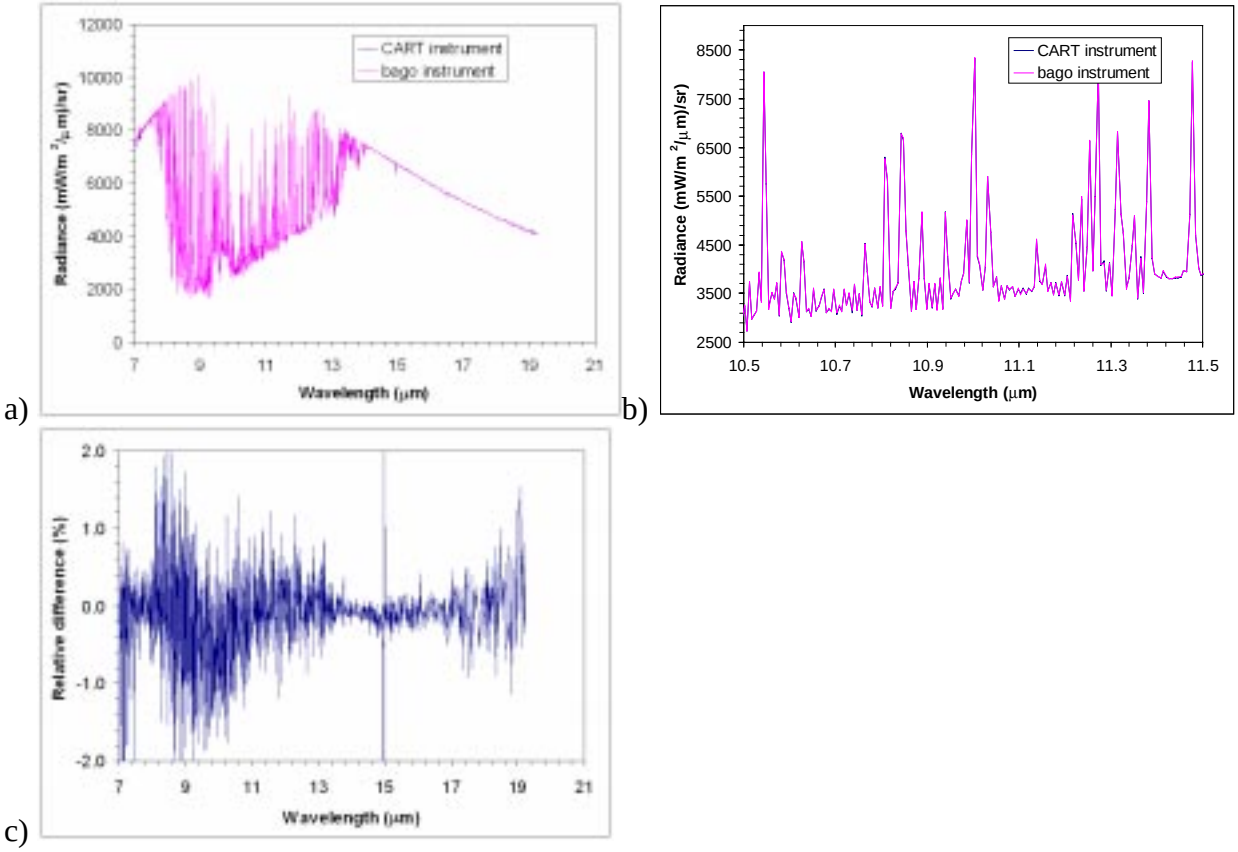

Figure 13 : Example of the radiometric accuracy achievable with a FTS

Figure 13 illustrates the radiometric accuracy achievable with FTS. The atmospheric spectra shown in Figure a) describe the downwelling radiance measured from the ground at the ARM Central Facility in Oklahoma using two independent AERI instruments operated by the University of Wisconsin (arm1.ssec.wisc.edu). An AERI is a non-imaging Bomem MB100 FTS equipped with a set of radiometric calibration sources and optimised optics to observe the atmospheric radiance under a 3-degree field of view. The calibrated spectra are obtained using a simple two-point calibration procedure (Revercomb et al., 1988) and no additional data manipulation (such as scaling) of the data is performed. Figure b) displays a small section of the radiance spectra and illustrate the detailed agreement of the two independent measurements (note that none of the features observed are due to noise). It is important to note that the spectral features are very narrow and of width comparable to the instrument lineshape function, which makes the inter-instrument comparison very sensitive to variation of lineshapes. The exceptional agreement of the small details demonstrates that FTS can not only be calibrated radiometrically with very high accuracy, but also spectrally in registration and

lineshape. Figure c) displays the percent relative difference of the spectra shown in a). The radiometric accuracy is better than 0.25 % for broad spectral features (around 14 and 16 mm) and at worse 2% (the average error being less than 0.5%) where considerable spectral structure is present.